Journal of King Saud University – Computer and Information Sciences 33 (2021) 161–182

Contents lists available at ScienceDirect

Journal of King Saud University – Computer and Information Sciences

journal homepage: www.sciencedirect.com

Analytical justification of vanishing point problem in the case of stairways recognition

Muhammad Khaliluzzaman

Dept. of Computer Science and Engineering, International Islamic University Chittagong (IIUC), Chittagong 4318, Bangladesh

ARTICLE INFO

Article history:
Received 21 October 2018
Revised 8 January 2019
Accepted 10 January 2019
Available online 14 January 2019

Keywords:
Computer vision
Vanishing point problem
Recognition system
Mathematical model
SVM
Uniform LBP

ABSTRACT

Stair region detection and recognition from a stair candidate image is a challenging work in the computer vision research area. In the last few decades, researchers use many recognition systems to recognize and verify the stair region from other analogous objects. However, all the verification systems such as vanishing point (VP) do not achieve the desired result for various reasons. In this regard, a method is proposed in this paper to investigate the vanishing point's problem arising in the case of stair region verification based on the three basic criteria, i.e. focal angle of the camera, height of the camera from the ground, and distance of the camera from the stair image. For that, primarily, the stair region is extracted by utilizing the geometrical features of a stair. The detected stair candidate region is verified through the y coordinate value of the vertical VP, i.e.$y < 0$. However, the y coordinate value of VP does not verify the stair region from all the scenarios. This paper investigates and justifies this problem utilizing the experimental analysis and introduces a mathematical model to estimate the location of the VP of the stair region. Finally, support vector machine (SVM) classifier is utilized instead of VP to recognize the stair candidate region and the performance of SVM is compared with respect to the VP. For that, rotational invariant uniform local binary pattern (LBP) is used for feature extraction. Stair images captured under different orientation and illumination conditions have been used to test the proposed method to evaluate the resultant accuracy.

1. Introduction

Appropriate object detection and recognition from a Red-Green-Blue (RGB) image is an important aspect and challenging task of the autonomous navigation system and computer vision. Detecting the stair position in a stair image is the analogous task. Detecting stairways region in a robust environment is the fundamental process for an intelligent autonomous navigation system (IANS) as well as for vision impaired people. For the real-time systems detecting a stair region is difficult for various stair shapes, different viewpoints, and non-uniform illumination conditions. For overcoming these difficulties and satisfy the needs of IANSs, the stair region detection and recognition process should be accomplished in the real-time as well as detect each target object from the stair image effectively. After detecting the stair candidate region, the detected region has to be verified through the verification methods. However, all the verification methods such as vanishing point (VP), do not work perfectly in all the scenarios and environmental conditions. Some verification methods perform better in specific scenarios and conditions. However, some methods are not performing better for various reasons such as different stair structures, and viewpoints. The reasons for which the problem occurs in the different verification method have to be investigated and justified.

In this regard, a method is presented in this work to investigate and justify the problem of a vanishing point which has occurred in the case of stair region recognition. For that, the stair candidate region is extracted by utilizing the geometrical features of a stair. One of them is every stair step's width is intersected with the ending points of the stair step horizontal edges, i.e. 3CP. The 3CP feature is presented in Fig. 1(a). This feature is used to validate the stair step's horizontal edges (HEs). Another feature is stair step's potential concurrent HEs appears in sorted order from bottom to top of the stair, which is shown in Fig. 1(b).

Peer review under responsibility of King Saud University.

Production and hosting by Elsevier

E-mail address: khalilcse021@gmail.com

https://doi.org/10.1016/j.jksuci.2019.01.004
1319-1578/

Fig. 1. Geometrical features of a stair: a) three connected point (3CP), and b) concurrent HEs are in sorted order

For satisfying these geometrical features, primarily, the input image is filtered by using a proposed multi-resolution singular value decomposition (MSVD) filtering procedure and resolute the stair step's edges, which is one of the key parts of the proposed method. After that, the concurrent HEs are extracted from the filtered image by utilizing the unexpected edge elimination and the edge linking procedure. The concurrent HE segment is validated by the aforementioned feature, i.e. 3CP. This validated edge segment is verified or recognized by the*y* coordinate value of vertical VP of the stair region, which is negative, i.e. $y < 0$. This process is shown in Fig. 2(a). This verification differentiates the stairways region from the diverse analogous objects such as a rail line as well as a pedestrian crossing, where, the VP of the analogous object is positive, i.e. $y \geq 0$. The processing examples of analogous objects are shown in Fig. 2(c) and (d).

The causes for which the variation of vanishing point occurs in the stair region or other analogous objects are hidden in their own structures. The main structural difference is that the rail-line and pedestrian crossing does not have a slope with respect to the ground, where the stair region is structured in such a way that it must have a slope with respect to the ground. However, this *y* coordinate value of VP does not recognize the different scenario's stair candidate regions for various reasons such as different stair structure and view point. Actually, whether the VP is located within or outside of the image plan depends on the slope and height of stair region. Where, the slope and height of a stair region in an image plan depends on the three basic criteria, i.e. 1) focal angle of the camera, 2) distance between camera and stair region, and 3) height of the camera from the ground. The effect of the basic criteria is shown in Fig. 2(e). These basic criteria are explained elaborately in Section 3.3. One of the examples is shown in Fig. 2 (b) image, which is the same image of Fig. 2(a) in the same environment. However, the focal angle and height of the camera from the ground are different. Here, Fig. 2(b) is captured with the bigger focal angle and higher height than the Fig. 2(a). For increasing the focal angle, the slope and height of the stair region in an image plan is decreased. On the same way, for increasing the height of the camera form the ground the slope and height of a stair region is also decreased. The effect of the focal angle and height of the camera on the Fig. 2(a) and (b) are shown in the Fig. 2(f) and (g) respectively.

From the above analysis, it is revealed that the focal angle and ground height of the camera are anti-proportional to the slope and height of the stair region. For these reasons, the VP of stair region located in Fig. 2(b) resides within the image plane, whichy coordinate value is positive, i.e. $y \geq 0$. In this case, the stair candidate region is not recognized by using the *y* coordinate value of VP. This paper investigates and justifies this issue with experimental analysis based on the three basic criteria. Afterward, a mathematical model is developed for estimating the location of VP of a stair region. This model is based on the ratio of stair region height and stair region ground height from the top of the image plane. This is another key contribution of the proposed method. Finally, the extracted stair candidate region is classified through an efficient classifier, i.e. SVM. Furthermore, the effectiveness of the SVM classifier is compared with respect to the VP. For that, the features of the stair candidate region are extracted by using the rotational invariant uniform local binary pattern (LBP).

The rest of the sections of this paper are demonstrated as follows. In Section 2 reviews the related work. The proposed method is explained step by step with processing examples in the next section. The processing examples, results, and discussion are presented in Section 4. Finally, Section 5 concludes the paper.

2. Related work

Over the past few decades, researchers have been proposed many stairways detection and recognition methods to overcome the research gaps. This section summaries some stair detection and recognition methods that have been implemented and tested previously. All the previous works concern a unique feature of a stair that is every stair edge image holds the consecutive parallel horizontal lines. Since the researchers and scientist have focused on the detection and recognition of a stair region, they have developed many improved stair detections and verification methods to raise the accuracy.

For example, some vision-based methods are introduced in Schwarze and Zhong (2015), Harms et al. (2015), Harms et al. (2014), Wang et al. (2014), Du Buf et al. (2011), Cong et al. (2008), and Basca and Brad (2007) to detect and recognize the stair candidate region. These methods utilize the stereo vision, mobile robot, smartphone, and unmanned ground vehicle (UGV) to navigate the stairways. Where, Wang et al. (2014) introduces a stair detection and recognition method based on the depth image. In this method, the stair is detected with the depth feature of the stair and is recognized by the SVM classifier. Some stair detection methods (Khaliluzzaman and Deb, 2018; Harms et al., 2015; Deb et al., 2013; Shahrabadi et al., 2013; José et al., 2012) are proposed based on the geometrical property of a stair. These methods are concerned with the geometrical features of a stair that are extracted from the stair edge image. A unique feature used in these methods

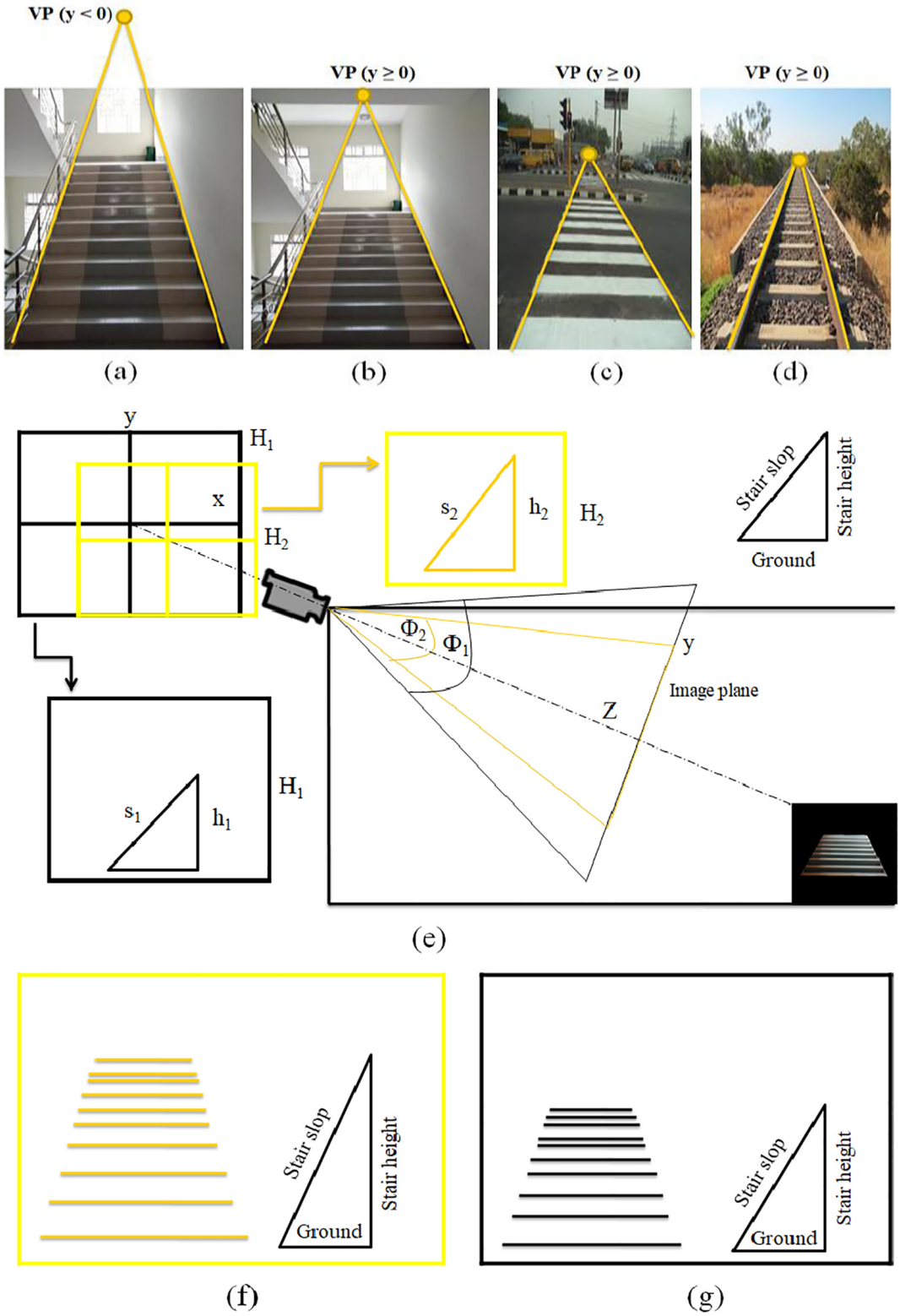

Fig. 2. Estimating the vanishing point from different structural objects: a) estimating VP from stair in a scenario where camera is focused to the stair region with low focal angle and the camera is not far away, in that situation the y coordinate value of VP is negative, i.e. $y < 0$, b) estimating the VP from a stair region in a scenario where the focal angle of camera is large and the height of the camera is higher than the camera by which Fig. 2(a) is captured, here, the y coordinate value of VP for the stair region is positive, i.e. $y \geq 0$, c) and d) estimating the VP from pedestrian crossing and rail line where the y coordinate value of VP for both of the objects are positive, i.e. $y \geq 0$, e) shows the effect of focal angle (Φ_1 and Φ_2) and height of the camera on the slope and height of the stair region based on the image plan (H_1 and H_2), f) and g) slope and height of stair region in the image plan for the Fig. 2(a) and Fig. 2(b) respectively.

is that every stair edge image contains consecutive parallel horizontal edges. Moreover, Harms et al. (2015) introduce a method where stair relevant edges are extracted through the Match filter. Afterward, the stair edge segment is determined from the relevant edges, and finally, this edge segment is used to detect the stair region.

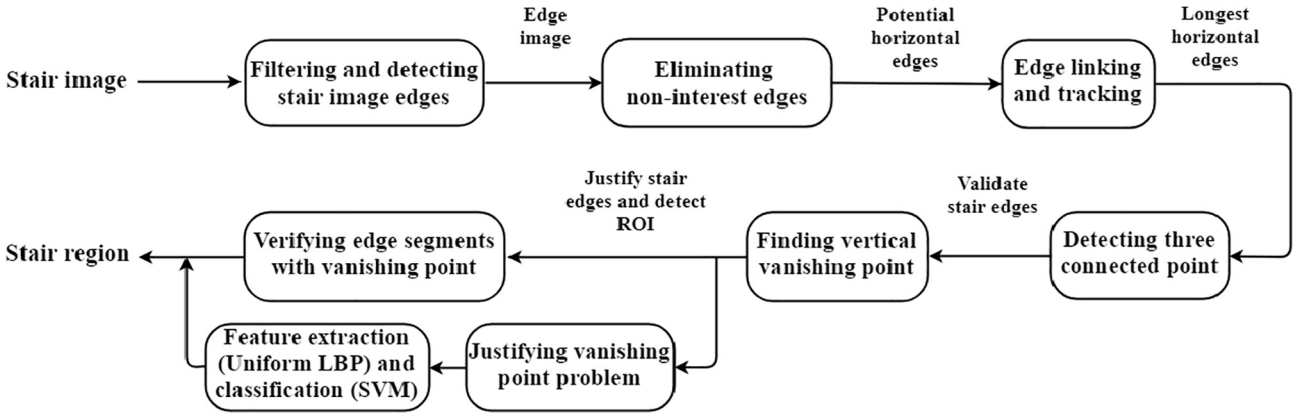

Fig. 3. Proposed stair detection and vanishing point problem justification method.

Earlier, the outdoor and indoor stair estimation procedure is introduced in Shahrabadi et al. (2013). This procedure accesses some criteria, i.e. white canes to detect the stair. In this algorithm, the camera is placed at a fixed distance from the stair, i.e. 5 m. Before that, a high accuracy and low false alarm rate framework for real-time stair detection is introduced in Lee et al. (2012). The AdaBoost learning algorithm is used in this framework. This framework improves the stair detection accuracy by extracting the features of three to four steps of a stair that are taken from the different conditions. The framework also improved accuracy by reducing the false positive rate.

Some constraint such as vanishing point (Schaffalitzky and Zisserman, 2000; McLean and Kotturi, 1995; Barnard, 1983) as well as a directional filter (Basca and Brad, 2007; Mäenpää and Pietikäinen, 2005) is used to localize and verify the stair region. Such as, Hernandez and Jo (2010) proposed a method, where the stair candidate region is initially identified by the vertical vanishing point. Then the directional Gabor filter is utilized for identifying the candidate area to extract the concurrent horizontal edges and detect the stair region. Later, an indoor localization method is introduced in Hernández et al. (2011). In this method, directional filter and planner motion tracking is used to detect and localize the stairways candidate region.

Furthermore, stair detection and verification frameworks based on the natural property of a stair and vanishing point is introduced in Khaliluzzaman and Deb (2018) and Deb et al. (2013). The natural property uses in Deb et al. (2013) is that the stair steps appear in sorted order from top to bottom of a stair by their length, where, Khaliluzzaman and Deb (2018) use the three connected point property of a stair. The longest increasing subsequence algorithm is used in Deb et al. (2013) to appear the concurrent horizontal parallel edges in sorted order. This problem is solved in $O(n \log n)$time, on the other hand, Khaliluzzaman and Deb (2018) introduce a method, where HEs are sorted by utilizing the x-coordinate value of HE segment end points. Finally, vertical VP is estimated from this sorted edge segment to verify whether this sorted edge segment is from stairways or any other stair likes object, i.e. rail line or pedestrian crossing. That is because of the rail-line and pedestrian crossing has analogous features as a stair.

Later, an earlier version of this paper (Khaliluzzaman and Deb, 2016) has introduced a method to identify the problem of VP during the stair region verification. However, this method is not efficiently justified the problem of VP. Here, the authors utilize the Gabor filter to eliminate the noise from the input RGB image, which is computationally expensive. Then the stair ROI is detected through the geometrical features of the stair. After that, the problem of VP is analysis with the y coordinate value of VP with simple stair samples. Complex and different oriented stair samples are not considered in this work. Finally, the stair ROI is verified by using SVM through the simple Gabor features.

In the previous research works, researchers utilized the vertical vanishing point to localize (Hernández et al., 2011; Hernandez and Jo, 2010) and recognize (Khaliluzzaman and Deb, 2018; Deb et al., 2013) the stair candidate region. However, in the different scenarios, the vanishing point does not work efficiently to localize and recognize the stair candidate region. The previous state of the arts such as Khaliluzzaman and Deb (2018), Deb et al. (2013), Hernández et al. (2011), and Hernandez and Jo (2010) are not focused on this issue. Such as, Hernandez and Jo (2010) proposed a framework, where the stair candidate region is initially localized from the outdoor environment by using the y coordinate value of vertical VP ($y < 0$). The other methods mentioned in Khaliluzzaman and Deb (2018) and Deb et al. (2013) verified the detected stair candidate regions by using the y coordinate value of VP ($y < 0$) that are captured form indoor and outdoor environments respectively. By this y coordinate value of VP, those methods differentiate the stair structural region from other analogous structural objects, i.e. rail line and pedestrian crossing. The example is depicted in Fig. 2. The causes for which variation of VP occurs in the different object regions are hidden in their own structures. The main structural difference is that, there is no slope with respect to the ground for the rail-line and pedestrian crossing, where, the stair region is structured in such a way that it must have a slope with respect to the ground.

In Khaliluzzaman and Deb (2018), Deb et al. (2013), Hernández et al. (2011), and Hernandez and Jo (2010) authors captured the stair image from the different environments by satisfying some conditions. The conditions are that the camera is placed in front of the stair with a height not more than two meters, and the camera is not placed so far away. If a stair image is captured from the long distance with the bigger focal angle and the height of the camera is higher from the ground, then the slope and height of the stair region will be smaller in the image plane. In those situations, the slope of the stair region is decreased and stair region is moved to the ground. As a result, the possibility is increased to reside the VP of the stair region in the image plane. In that case, the y coordinate value of VP will be positive in the image plane i.e., $y \geq 0$, which is shown in Fig. 2(b). For that reasons, the stair region cannot be localized and verified by utilizing the y coordinate value of VP. This problem is not considered in these mentioned methods, where, the y coordinate value of VP is used to localize and verify the stair region.

In this paper, we have focused on this issue and justify the vanishing point problem experimentally by considering the three basic

criteria, i.e. focal angle of the camera, height of the camera from the ground, and distance of the camera from the stair image. Finally, a mathematical model is developed to predict the location of VP of a stair region.

3. Explanation of the proposed method

The proposed framework is primarily divided into four major parts, that are, (1) applying MSVD for filtering and extracting the edge information, (2) detection of stair candidate region and verifying by using vertical VP, (3) justifying the VP problem in the case of stair region localization and verification, and (4) feature extraction and classification.

The stair ROI detection and verification process has some basic steps that are, (1) removing unexpected edges from edge image, (2) estimate the potential HEs using edge linking, (3) identifying geometrical features in potential HE segment and detect the stair ROI, and (4) verifying and detecting stair candidate region by VP. The framework is depicted in Fig. 3.

3.1. Applying MSVD filter and detection edge information

The fundamental step of any computer vision and image processing framework is to eliminate the noisy information from the input image that is captured in the phase of image acquisition. Moreover, stair region is located in the environments where noises and shadows affect are added in the stair candidate region.

The main problem for reducing the noises from an image is to separate the noise and original values from the image. For that, in this work, a multi-resolution singular value decomposition (MSVD) filtering procedure is utilized for image de-noising, which is similar to the wavelet transform (WT) (Naidu, 2011; Hou, 2003; Mallat, 1989). In WT, the input image is decomposed into four sub-bands, which are achieved through the sub-band filtering, i.e., finite impulse response (FIR) filters. The first sub-band in WT contains low frequency and high amplitudes details, i.e. approximation subband (LL). Other three sub-bands are contained the low amplitudes and high-frequency details. In MSVD, the FIR filters are replaced with the singular value decomposition (SVD). The SVD of m × n image is defined in Eq. (1).

$$X = USV^T = \sum_{i=1}^{N} u_i s_i v_i^T \tag{1}$$

here, U and V is the nxn and mxm orthogonal singular matrix respectively. U is the Eigen column vector of $T = XX^T$ that brings the diagonal matrix $U^T TU = S^2$, where, S is the m × n diagonal descending singular matrix, which is also known as Eigen value of XX^T.

To convert the image X into four sub-bands, the image X has to reshape $4 \times m/2 * n/2$ image which is define as X_1. And apply SVD on the reshape X_1 image to bring the Eigen vector U. So, the Eigen column vector U will be 4×4 matrix i. e., $\{E_k\}_{k=1}^{4}$ from the basis for the space $\mathbb{R}^n$.

In addition, when image X is reshaped into X_1, which is $4 \times m/2 * n/2$, it does not maintain the scaling factor. So, the original image information will be destroyed. For that, a modified reshape method is applied to input image X to reshape into X_1. The method is explained in the procedure that is given bellow.

Procedure 1: Modified image reshaping procedure
X: Input Image which is m × n size.
X_1: Reshape image which will be $4 \times m/2 * n/2$ size
B: 4×4 size block image taken from image X to reshape
C: Indicate the column of X_1 in which reshape of B will put
For i = 1 to m/2
For j = 1 to n/2
C = j + (i−1) * m
$B = \left[\{X_r\}_{r=(j-1)*2+1}^{(j-1)*2+2}, \{X_c\}_{c=(i-1)*2+1}^{(i-1)*2+2}\right]$
Take block B from image X, reshape into
4×1 sizes and put into C columns of X_1
End
End

Each $\{E_k\}_{k=1}^{4}$ represents the specific sub-band Eigen vector of X_2. To extract the four specific sub-bands (LL, LH, HL, HH) from the reshape image X_1, which is $4 \times m/2 * n/2$ using Eigen vector U i.e., $\{E_k\}_{k=1}^{4}$, performs the operation $X_2 = U^{-1}X_1$. The resultant matrix X_2 will be also $4 \times m/2 * n/2$ matrix. In that matrix, each row represents a specific sub-band. The first row i.e. $X_2(1, :)$ contains the low frequency and high amplitude information, that are the most approximation information which corresponds to the largest Eigen value, i.e. LL. The rest of the rows represent the high frequency information that corresponds to the smallest Eigen values, i. e. LH, HL and HH. The first row information $X_2(1, :)$, i.e., LL is taken as a filtered image and reshape in m × n size. The filter effects on the stair image are shown in Fig. 4(b), where, the input RGB image is shown in Fig. 4(a).

To satisfy the geometrical features of a stair, i.e. 3CP and the potential HEs are in sorted order, the stair steps potential HEs, and the vertical edges at the HEs ending regions are required. For that, the Canny operator (Cortes and Vapnik, 1995; Huertas and Medioni, 1986) is utilized to extract the stair edges through the

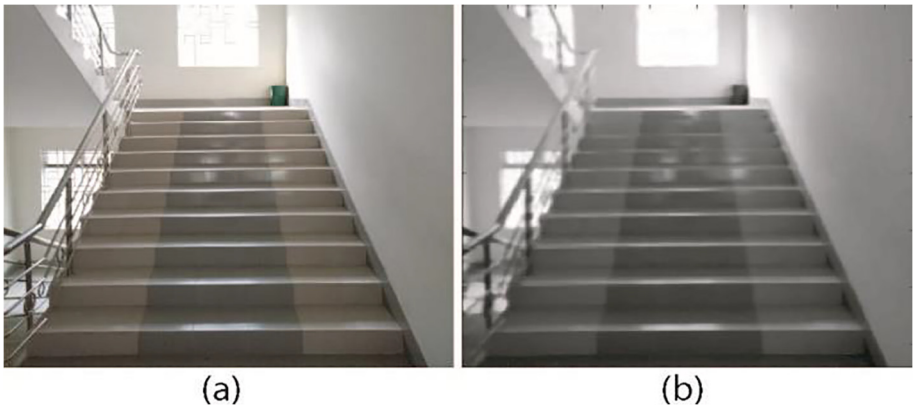

Fig. 4. Filtering process: a) input RGB stair image, b) MSVD filtered image.

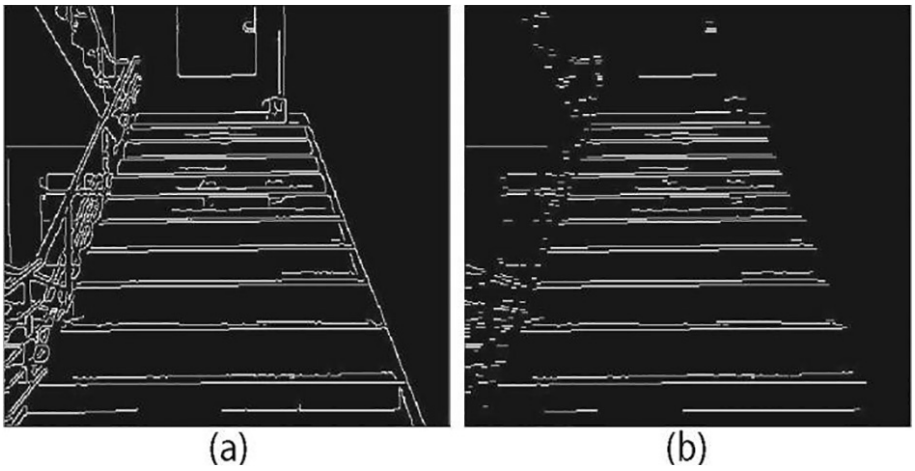

Fig. 5. Edge extraction process: a) edge image extracted by the Canny operator, and b) eliminating vertical edges to extract the horizontal edges.

step characteristics. This is because of the Laplacian operator such as Canny operator has the advantage of smoothing to reduce the Gaussian noise and has the thresholding method by which stair edges can be detected efficiently. The key feature of the Canny operator is its ordinary attributes. The attributes are threshold values (Huertas and Medioni, 1986) and the standard deviation.

The boundary of an object usually produces by the step edges, as the image intensity of an object is different from the image background. Accordingly, in the steps of the stair, the intensity value is changed rapidly and the intensity in the stair steps height and its width is different. So, the edges of the stair can be extracted through the step characteristics. The outcome of the Canny operator with step characteristics is presented in Fig. 5(a).

3.2. Detecting and verifying stair ROI

The detection process of a stair candidate region is explained in this section. The process requires some basic steps, i.e., (1) removing unexpected edges from the edge image, (2) extracting potential HEs through edge linking, (3) identifying geometrical features in potential HE segment and detect the stair ROI, and (4) verifying and detecting stair candidate region by VP.

3.2.1. Removing unexpected edges

To detect the stair candidate region the proposed method needs to extract the potential horizontal and vertical edges. However, in the Canny edge image, many unexpected edges exist in the different orientation. For this regard, initially, HEs are extracted from the Canny edge image by removing the VEs. The extracted horizontal edges are shown in Fig. 5(b). In Fig. 5(b), it is seen that HE image contains a lot of small non-candidate edges. That non-candidate HEs are eliminated from the Canny horizontal edge image through a filtering method. According to the filtering method, the edges those are smaller than a statistical threshold value will be removed from the HE image.

The statistical threshold value is defined as $\sqrt{\frac{\sum_{i=1}^{N}(edge(i)-edge_mean)^2}{N}}$, that is the edge values first standard deviation exist in the Fig. 5(b). Here, N represents the total number of HEs. The small edge removing procedure outcomes is shown in Fig. 6(a). In Fig. 6(a) still exists various HEs that are not parallel to the potential concurrent HEs. Those non-parallel HEs are removed from the edge image as unexpected edges are presented in Fig. 6(b).

3.2.2. Edge linking and extracting potential HEs

The HE image mainly contains the longer horizontal step edges. These HEs may have breaks or gaps in various areas. These breaks or gaps are necessary to be filled up for extracting longest horizontal edges that convey the information of the stairway region. In this work, a method is proposed to make up the breaks or gaps. According to the method, the breaks or gaps of three pixels are makeup automatically. On the other hand, the linking procedure will be

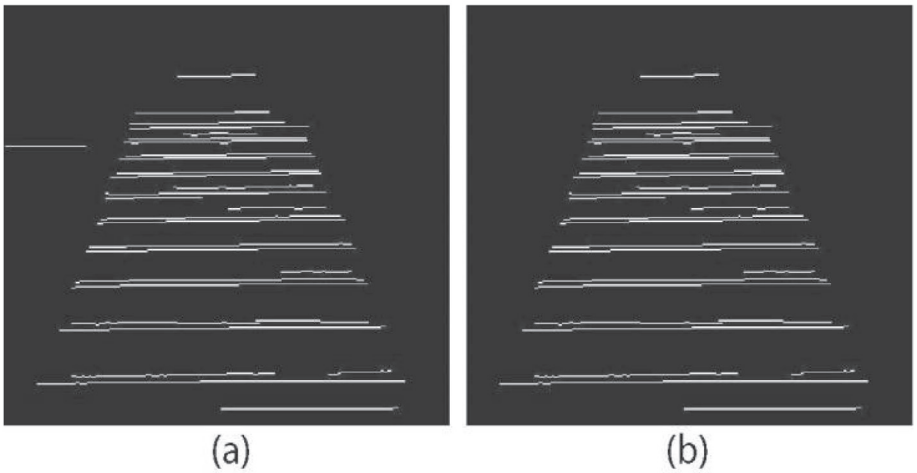

Fig. 6. Unexpected edge elimination process: a) eliminating small HEs b) filtering unexpected edges.

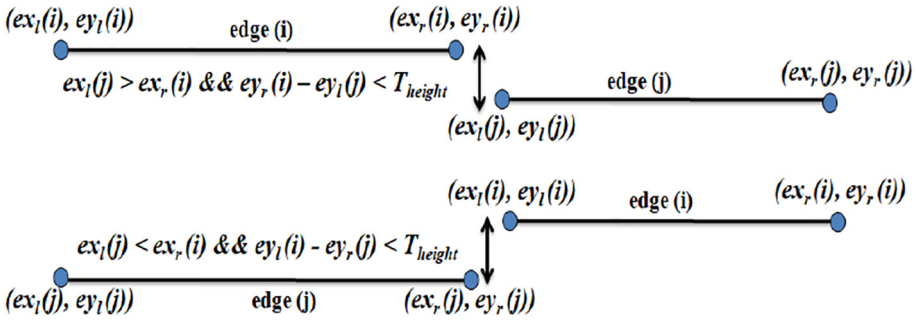

Fig. 7. The process of edge linking.

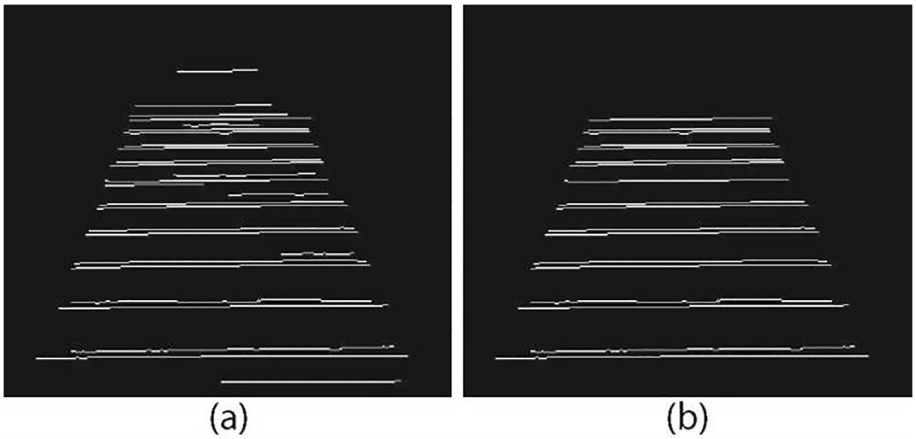

Fig. 8. Edge linking and potential edge extraction process: a) edges linking outcome, and b) filtering unnecessary edges within the concurrent edge segment.

applied that is shown in Fig. 7. According to the process described in Fig. 7, the right point of edge (i) i.e.,($ex_r(i)$, $ey_r(i)$) is linked to the left point of edge (j) i.e., (ex_l(j), $ey_l(j)$) if these points satisfy the following conditions i.e., $ex_l(j) > ex_r(i)$ as well as $ey_r(i) - ey_l(j) < T_{height}$. The right point of edge (j) i.e., ($ex_r(j)$, $ey_r(j)$) is linked to the left point of the edge (i) i.e., (ex_l(i), $ey_l(i)$) if these points satisfy the following conditions i.e., $ex_r(j) < ex_l(i)$ as well as $ey_l(i) - ey_r(j) < T_{height}$. Where, ex_r, ex_l are x coordinate and ey_r *and* ey_l are y coordinate of the left and right end points of horizontal $edge(i)$ and horizontal $edge(j)$ respectivelly.

In this procedure, a statistical threshold (T) is considered. The threshold value is the one-third of the average height of the longest potential HEs. The edge linking outcomes are demonstrated in Fig. 8(a). Still, the linked edge image contains the many unnecessary small edges. These unnecessary edges are located within the concurrent edge segment.

Those unnecessary horizontal edges are dispelled from the edge image through a statistical model, i.e., the edges which consecutive edge value difference is less than the statistical threshold value will be eliminated from the edge image. The threshold value is estimated by using mean absolute deviation (MAD) that is$\frac{\sum_{i=1}^{N}|edge(i)-edge_mean|}{N}$. The outcome is shown in Fig. 8(b). Where, the longest potential horizontal edges are only existed. Let the total number of potential HE is N.

3.2.3. Identifying geometrical features and detecting the stair ROI

For identifying the expected stair region from the horizontal edge image the basic geometrical features of a stair are used. The main geometrical feature used in this work is three connected point (3CP), i.e., every stair step's width is intersected with the ending points of the stair step's HEs. Another geometrical feature

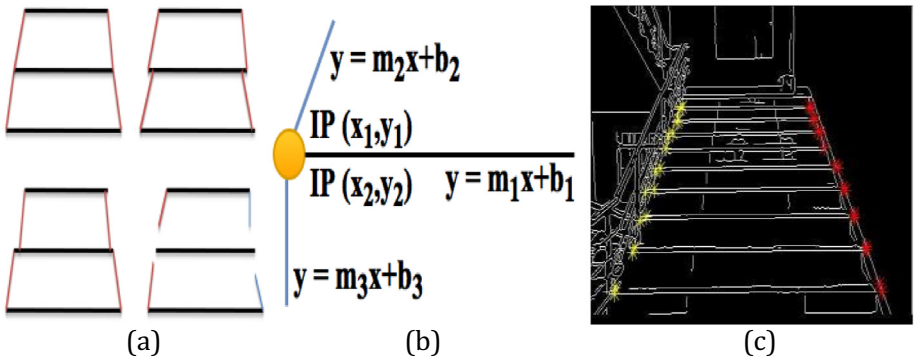

Fig. 9. The process of geometrical feature estimation: a) different variation of vertical and horizontal edges, b) procedure of estimation 3CPs, and c) 3CPs in the edge image.

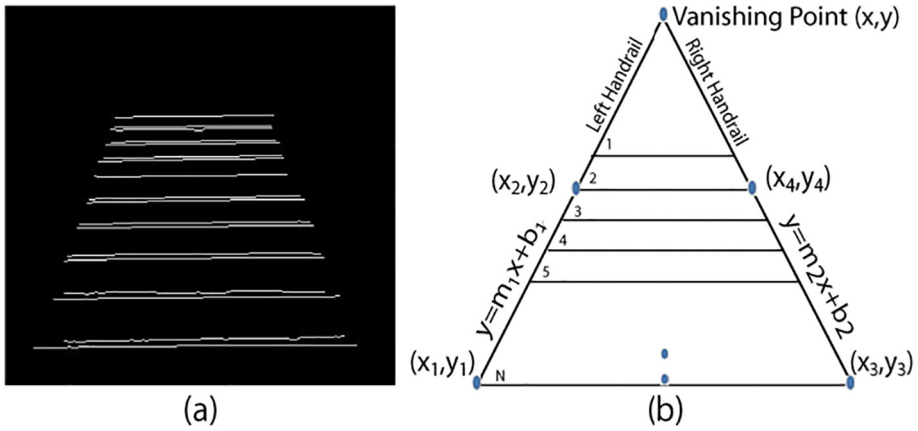

Fig. 10. HEs extraction and estimation VP: a) appears HEs are in sorted order, and b) procedure of estimating vertical VP.

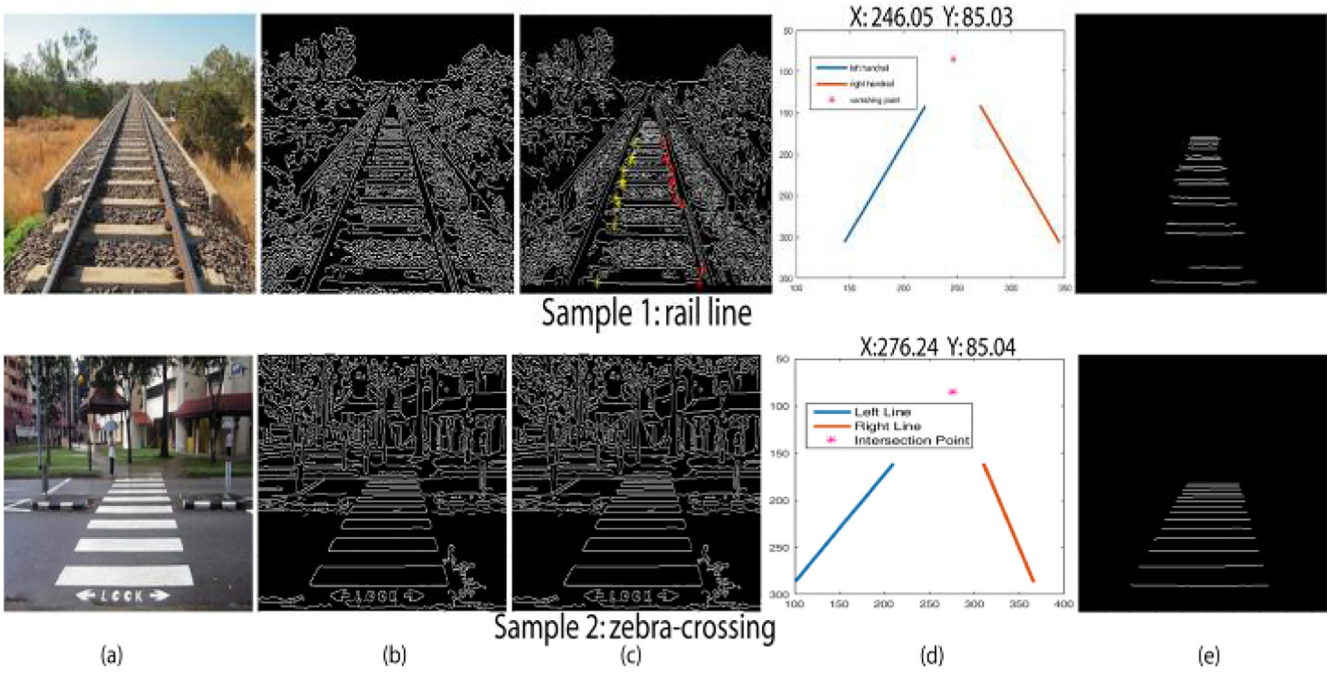

Fig. 11. Processing example of stair analogous objects: a) input RGB image, b) extracted Canny edges, c) HEs validated by 3CPs, d) estimating the vanishing point, and e) HEs are in sorted order.

used in this work is stair step's concurrent HEs appear in sorted order. These features are shown in Fig. 1.

By these geometrical features, the previously extracted potential HEs are validated and justified. For that, the ending points of the potential HEs are searched to find the vertical width edges. This operation is performed to estimate the 3CP by which the potential HEs are validated. However, the VEs and HEs are not all time exactly vertical or horizontal for different noise and illumination conditionals, that are shown in Fig. 9(a). The recovery process of estimating 3CP is shown in Fig. 9(b). Where, the two vertical edge lines are presented as $y = m_2x + b_2$ and $y = m_3x + b_3$ and the horizontal edge line is presented as$y = m_1x + b_1$. Here,m_1, m_2, andm_3 are the slope of the horizontal and vertical edge lines. From horizontal edge line $y = m_1x + b_1$ and vertical edge line $y = m_2x + b_2$ the first intersection point(x_1, y_1) is estimated. The second intersection point (x_2, y_2) is estimated from the horizontal line $y = m_1x + b_1$ and vertical edge line$y = m_3x + b_3$. From these two intersection points the three connected point is estimated. The outcome of the applying the process to estimate the 3CP on the stair edge image is presented in Fig. 9(c).

According to the procedure that is presented in Fig. 9(b), it requires a constant time to estimate the one 3CP at each ending points of HE. Let, the time is C. So, for finding two 3CP at each HE's ending points required *2C* time. For estimating 3CPs from the *N* HEs need the *2NC* time. So the final time complexity will be raised as *O(N)*.

After estimating the 3CP from the previously extracted N horizontal edges, the system validates whether the extracted N horizontal edges are from stair or not. This validation is confirmed if the estimated 3CP is more than 75% with compare to the previously extracted N horizontal edges.

The validated edge segment is shown in Fig. 10(a). Furthermore, the potential HEs that are validated by 3CP are checked by the VP to confirm that the extracted edges are from stair or from the other visually similar object, i.e. rail line and pedestrian crossing. That is because of, the rail line and pedestrian crossing have the analogous

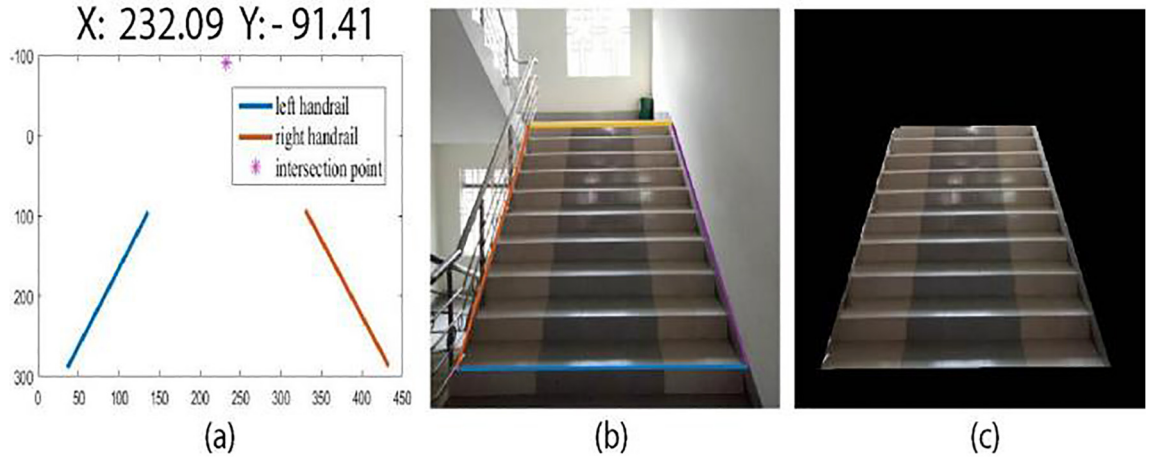

Fig. 12. Detecting stair candidate region: a) estimating VP, b) figure out the ROI in the input stair RGB image, and c) detected stair candidate ROI.

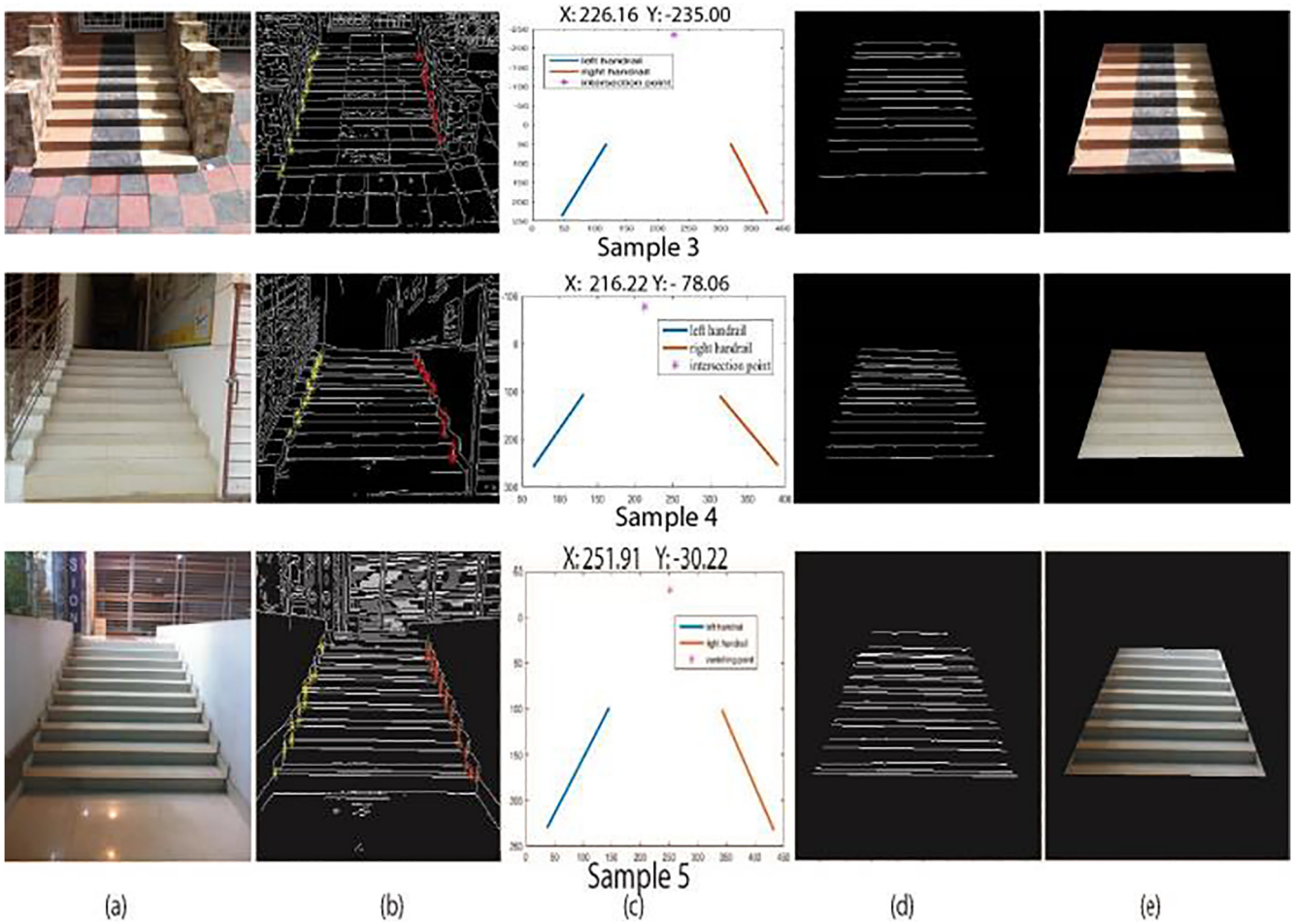

Fig. 13. Processing example of stair region detection by geometrical feature and verified by vertical VP: a) input stair RGB image, b) HEs validated by 3CPs, c) estimating the vanishing point, d) HEs are in sorted order, and e) extracted stair candidate ROI.

features as a stair. The VP point is the imaginary point intersected by the two straight lines. In this work, VP is determined by the straight lines that are passed through the 3CPs at the ending side of the HEs. The process of estimating VP is presented in Fig. 10(b).

From the Fig. 10(b) it is observed that, if the vanishing point is determined from the potential HE segment that is validated through the 3CP, then the edge segment is appeared in the sorted order from bottom to top of the stair, which is another geometrical feature of the stair. This feature justifies that the detected potential HE segment is extracted from the stair region, which is the stair candidate ROI.

3.2.4. The stair candidate region is verified by the vertical vanishing point

The detected stair ROI in verified through the vertical vanishing point. For that, the *y* coordinate value of VP is utilized. The reason

behind that, the y coordinate value of the VP that is estimated from the stair will be negative ($y < 0$). This value will be remaining in the range of $-2IH \leq YCVP < 0$. Where, IH and $YCVP$ are represent the image height and the y coordinate value of VP respectively. The confirmation of extracting ROI is from stair or not is defined by the conditions mentioned in Eq. (2).

$$ROI = \begin{cases} From\ stair, & if \quad YCVP < 0 \\ From\ another\ similar\ object, & if \quad YCVP \geq 0 \end{cases} \tag{2}$$

If the VP of the ROI is not satisfied with the condition mentioned in Eq. (2), then the parallel HEs are not certain as the stair step edge segment. These concurrent parallel HE segments were estimated from other stair analogous objects such as rail line or pedestrian crossing. The reason behind that, both the rail line and pedestrian crossing have the analogous visual features as a stair. The main difference is that the y coordinate value of VP determined from the rail line and pedestrian crossing will be positive i.e. $y \geq 0$.

The processing experiment result for the rail line and pedestrian crossing is shown in Fig. 11. According to the experiment, it is seen that both the rail line and pedestrian crossing satisfy the analogous feature of the stair.

However, the VP determined from the pedestrian crossing and rail line are different, i.e., (246.05, 85.03) and (274.29, 73.22) is represented in Fig. 11(d).

Here, the y coordinate value of VP for pedestrian crossing and rail line are 85.03 and 73.22 which are positive, i.e. $y \geq 0$. These y coordinate values of VP differentiate the stair region from the analogous objects such as pedestrian crossing and rail line. The causes for which the vanishing point's variation occurs in the stair region or other analogous objects are hidden in their own structures. The main structural difference is that the rail line and pedestrian crossing's structure do not have any slope with respect to the ground, where, the stair region is structured in such a way that it has a slope with respect to the horizontal axis, i.e. ground. So why, the VP of the stair region is formed outside of the image, i.e. negative ($y < 0$).

The detected VP from the stair ROI is shown in Fig. 12(a), where, the y coordinate value of VP is −91.41. The detected stair region in stair RGB stair image is as presented in Fig. 12(b). Where, Fig. 12(c) shows the detected stair candidate region.

This section explains some processing example to justify the stair region verification through the VP, where, the stair candidate region is detected by using the geometrical features of a stair. To satisfy the verification by using the VP, the stair image is captured from the different scenarios with some specific conditions. The conditions are that the image is captured with a height from the ground that is not more than two meters, and the distance from the stair to the camera is not so far away. The focus of the camera should be navel to the stair region. Some experiments are shown in Fig. 13.

The samples presented at the Fig. 13 are taken from different scenarios and environmental conditions to justify the effectiveness of the proposed system. Such as, stairways Sample 3 is taken from the outdoor scenario at daytime. Where, Sample 4 and 5 are taken at the uneven illumination conditions both are from indoor and outdoors respectively. All the samples presented at the Fig. 13 validate the geometrical features of the stair, i.e. 3CP and HEs appears in sorted order. These images are also verified by the y coordinate value of VP, i.e. $y < 0$. These experimental values including processing execution time is presented at Table 1.

3.3. Investigating and justifying the vanishing point problem

The problem of a vanishing point for the stair region verification is investigated in this section. This problem occurs in the situations when the stair image is taken in such a way that the camera is not closely focused to the stair region, and the slope and height of the stair candidate region is low in the image plane. In those situations, the VP of stair region will reside within the image plane. That means the y coordinate value of VP will be positive, i.e., ($y \geq 0$) and it is not located within the range of $-2IH \leq YCVP < 0$, where, IH is the image height and $YCVP$ is the y coordinate of the VP. As the VP does not satisfy the condition presented in Eq. (2), hence,

Table 1
Validated stair step HEs by 3CPs, estimating VP value and the processing time of sample images.

Stair sample	Total HEs	Total 3CPs	3CPs (%)	Vertical VP	Run time (s)
3	15	12	80.00	(226.16, −235.0)	0.056
4	15	12	80.00	(216.22, −78.06)	0.056
5	18	16	88.89	(251.91, −30.22)	0.062

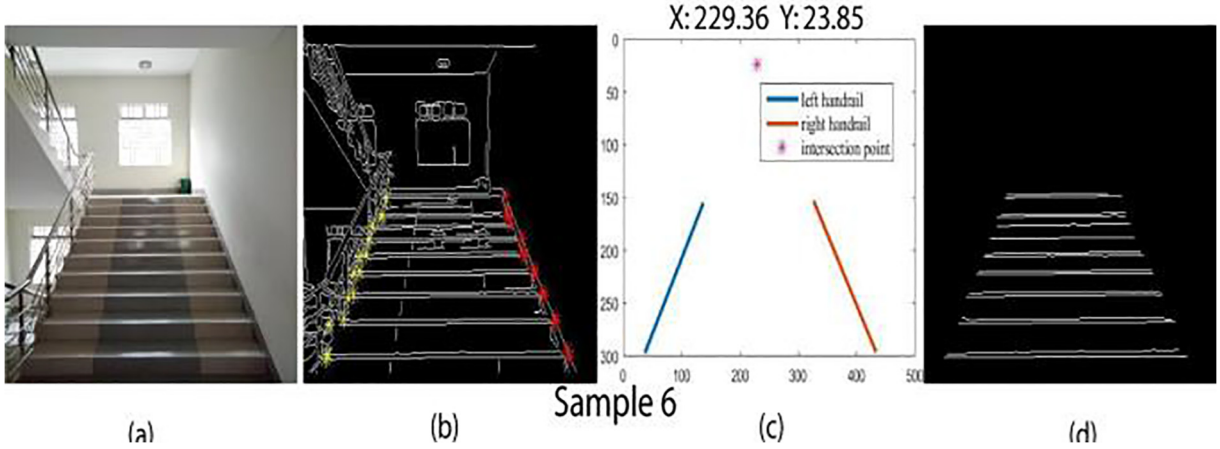

Fig. 14. Processing example for identifying the problem of VP: a) input stair RGB image, b) HEs validated by 3CPs, c) estimating the vanishing point, where, y≥0, and c) HEs are in sorted order.

the stair candidate region is misclassified as a rail line or pedestrian crossing. The problem of vanishing point with the experimental result is shown in Fig. 14. The image presented in Fig. 14 is the same image of Fig. 4(a), however, the image Fig. 14 is captured with a large focal angle, and the higher height from the ground. From the Fig. 14, it is revealed that the stair region is satisfied with the condition of the geometrical features. However, the *y* coordinate value of VP of that sample is positive ($y \geq 0$), i.e. 23.85.

3.3.1. Analytical justification

Actually, whether the VP is located within or outside of the image plane is dependent on the slope and height of the stair region in the image plane. Basically, the slope and height of the stair region in an image plane depends on the three basic criteria, i.e. 1) focal angle of camera, 2) distance between camera and stair region, and 3) height of camera from the ground. The justifications of VP problem based on these three basic criteria are demonstrated in Figs. 15–17.

In Fig. 15 the basic criteria of focal angle is explained, here, the same image is captured with the two different focal angles (Φ_1 and Φ_2) and these images are placed in the two 2D image planes which heights are H_1 and H_2. As the angle of Φ_1 is bigger than the Φ_2, the image plane H_1 for Φ_1 (black color) is bigger than the image plane H_2 for Φ_2 (yellow color) where the same size of stair region is captured.

From these analyses, it is revealed that, if the image is captured with a large focal angle then the slope and height of a stair region in a image plane will be smaller, which is anti-proportional. If the focal angle is more increased then the slope of the stair region will be more decreased, and the stair steps are going to be more parallel to the ground. So why for the large focal angle the VP of the stair region will reside in the image plane, which is shown in Fig. 15 (b). Accordingly, for lower focal angle (Φ_2), the slope (s_2) and height (h_2) of stair region in the image plane will be bigger. Here, the height ratio of the stair region (h_2) and the image plane (H_2) is bigger than the ratio of h_1 and H_1. Hence the VP for that stair region will reside outside of the image plane, which is shown in Fig. 15(c).

The effect of camera's distance criterion for evaluating the VP of stair region is explained in Fig. 16. Here, the same stair image is captured from the different distance point A and B with different focal angle Φ_1 and Φ_2. These captured images are placed in the two 2D image planes which heights are H_1 and H_2. From the Fig. 16, it is observed that the image plane H_1 i.e., captured from point A is bigger than the image plan H_2 i.e., captured from point B. It is also observed that the slope (s_1) and height (h_1) of the stair region in the image plane are smaller if the image is captured from the large distance and vice versa. That means the relation between the slope and height of stair region is anti-proportional to the distance of the camera form the stair region.

The relation between the slope and height of stair region based on the distance of the camera is shown in Fig. 16(d), where, black and yellow color horizontal edges appear from the stair regions that are captured from the long and short distance respectively. Here, slope and height are explained with the stair step's horizontal edges for the better understanding. Form Fig. 16(d), it is revealed that the edge slope of stair steps is decreased if the distance of the camera from the stair region is increased. If the distance between the camera and the stair region is more increased then the horizontal stair-step edges will be more parallel to the ground, which increases the possibility to reside the VP of stair region within the image plane.

Camera's long-distance effect on the slope and height of the stair region in the image plane is shown in Fig. 16(b). The short distance effect is shown in Fig. 16(c). Form Fig. 16(b), it is seen that for long distance the slope (s_1) and height (h_1) of stair steps are decreased and the horizontal parallel edges of stair steps are moved to the ground. As a result, the VP of this parallel edge segment resides within the image plane, and the *y* coordinate value of the VP will be positive, i.e. $y \geq 0$, which is shown in Fig. 16(b). On the other hand, for the shorter distance, the slope and height of

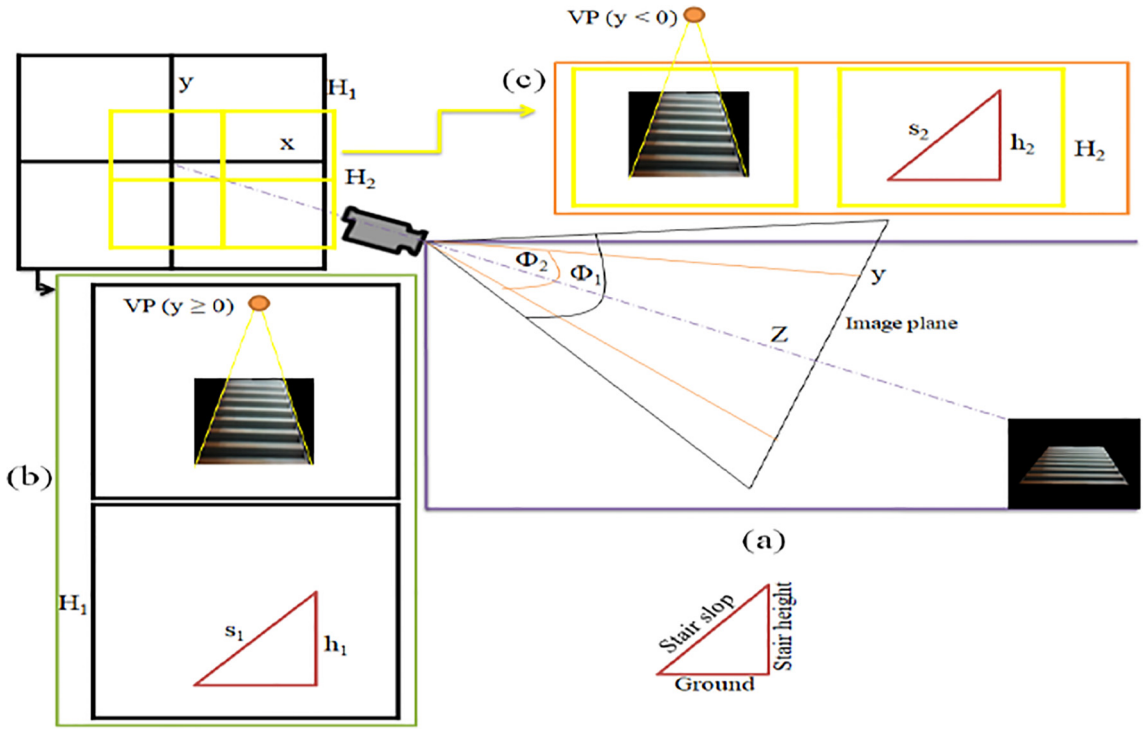

Fig. 15. Explanation of the VP problem based on the focal angle criteria: a) image plane in different focal angle, b) stair image in the image plane with Φ_1 focal angle, and c) stair image in the image plane with Φ_2 focal angle.

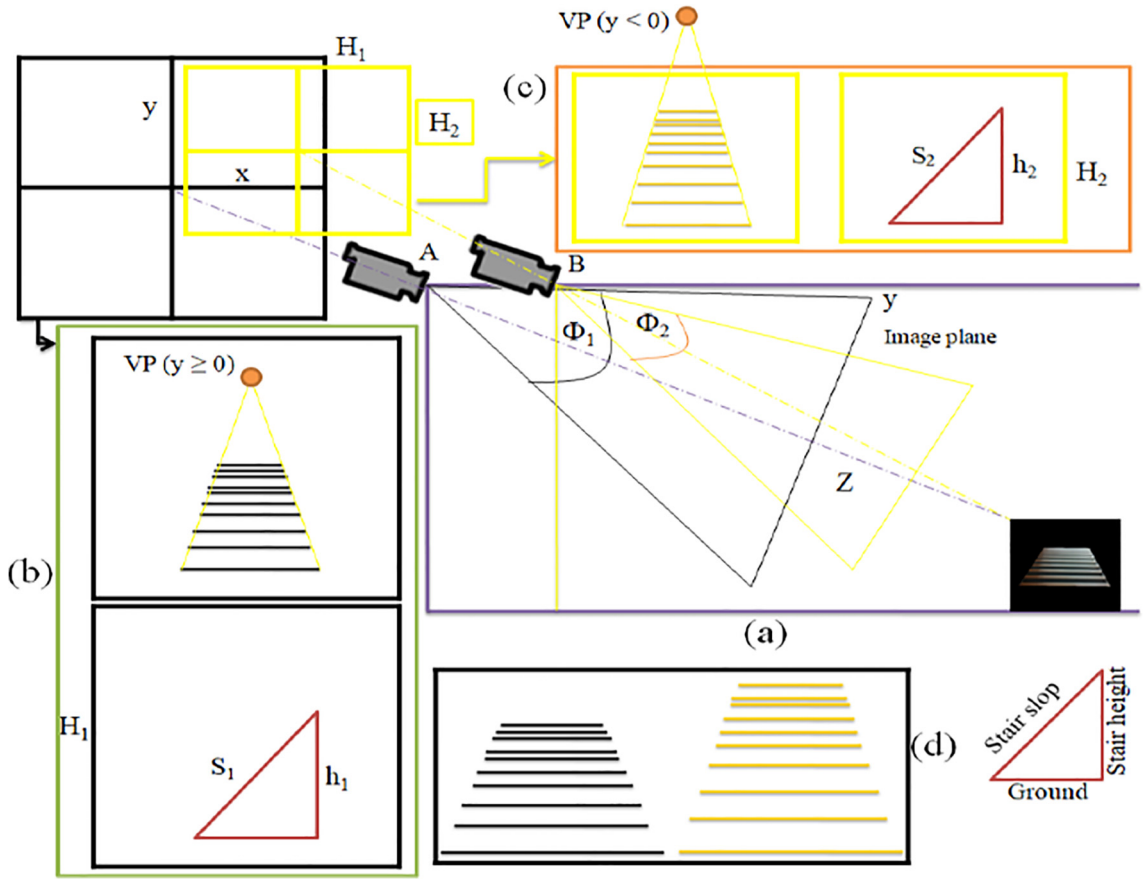

Fig. 16. Explanation of the VP problem based on the criterion of distance between camera and stair region: a) image plane in different distance, b) stair image in image plane captured from long distance with Φ_1 focal angle, and c) stair image in image plane captured from short distance with Φ_2 focal angle, and d) comparison of stair steps slope and height captured from different distance (Black color captured from the long distance and yellow color captured from the short distance). (For interpretation of the references to color in this figure legend, the reader is referred to the web version of this article.)

stair region will not be decreased as like the long distance, which is shown in Fig. 16(d). In the short distance, the slope (s_2) and height (h_2) of stair steps is bigger than the slope (s_1) and height (h_1) of the long distance. From Fig. 16(c), it is also observed that the ratio of stair step's height (h_2) and image plane height (H_2) is considerably large with respect to the ratio of h_1 and H_1. As a result, the VP of that stair steps edge segment is resided outside of the image plan, which is shown in Fig. 16(c).

The effect of the camera's height criterion for evaluating the VP of stair region is demonstrated in Fig. 17. To describe this criterion same image is captured from the same distance with different heights AC and BC. These images are placed in the two 2D image plane which heights are H_1 and H_2.

Since the images are captured from the same distance, so the image plans H_1 and H_2 are almost the same. However, the projection of the stair region in the image plane is not the same. The projection of stair region in the image plane is different due to the height of the camera from the ground. The stair steps edge segment's slope and height for long (black color) and short (yellow color) distance are presented in Fig. 17(d). From Fig. 17(d), it is revealed that for increasing the height of the camera from the ground the slope and height of the stair region in the image plane will be decreased. That means the relation between the slope and height of the stair region is anti-proportional to the height of the camera from the ground and vice versa.

If the height of the camera is more increased then the projection of the stair step's horizontal parallel edges will be more parallel to the ground and increase the possibility to reside the VP of stair region within the image plane. The effect of the height of the camera on the stair region for estimating VP is shown in Fig. 17(b) and Fig. 17(c). From the Fig. 17(b), it is seen that for higher height (BC) of the camera the stair steps parallel horizontal edges are moved to the ground and decreased the stair steps slope (s_1) and height (h_1). As a result, the VP of this edge segment resides within the image plane, which y coordinate value of the VP is positive, i.e. $y \geq 0$. Where, in Fig. 17(c), for the lower height (AC) of the camera, the stair steps horizontal edges show the higher slope (s_2) and height (h_2) in the image plan and the ratio of stair step's height (h_2) and image plan height (H_1) is considerably large. As a result, the VP of that stair steps edge segment is resided outside of the image plane, which is shown in Fig. 17(c).

3.3.2. Mathematical model for estimation VP's location

From the analysis of the three basic criteria, it is clear that whether the VP of a stair region is located within or outside of the image plane depends on the slope and height of stair region. However, exactly which condition the VP will reside within or outside of an image plane is not explained in the basic criteria section. In this regard, a mathematical model is introduced in this section to estimate the location of the vanishing point of a stair region.

According to the three basic criteria, the location of the VP of a stair region in the image plane is dependent on the stair region's height, and the placement of the stair region in the image plane. Therefore, predicting the location of the VP of a stair region, a mathematical model is established in this section. This model is based on the ratio of stair region's height and stair region's ground height from the top of the image plane. The VP's location estimation procedure is demonstrated in Fig. 18.

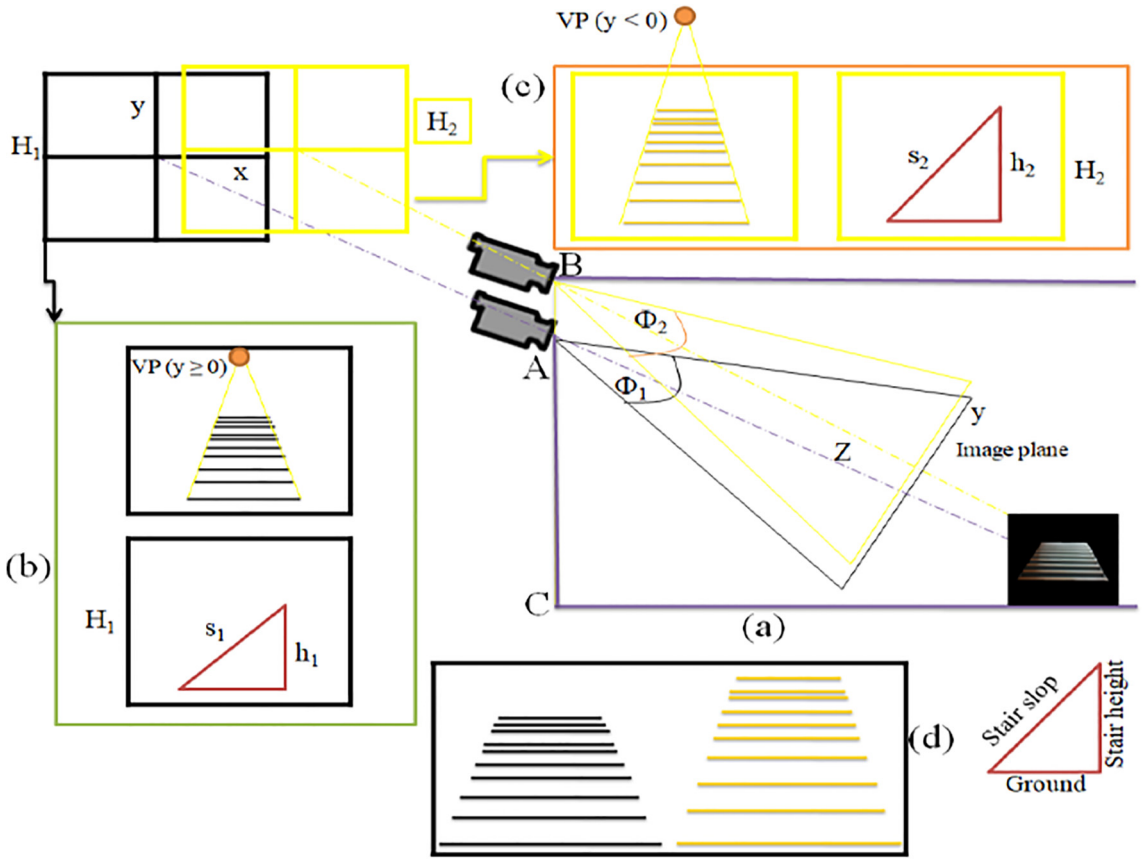

Fig. 17. Explanation of the VP problem based on the criterion of height of the camera from the ground: a) image plane in different height from the ground, b) stair image in image plane captured from height AC with Φ_1 focal angle, and c) stair image in image plane captured from the height BC with Φ_2 focal angle, and d) comparison of stair steps slope and height captured from different height (Black color captured from height AC and yellow color captured from height BC). (For interpretation of the references to color in this figure legend, the reader is referred to the web version of this article.)

According to the procedure shown in Fig. 18, the vanishing point $P(x_p, y_p)$ is formed by the intersection of the two straight lines AP and CP. The straight lines AP and CP are passing through the points $A(x_1, y_1)$, $B(x_2, y_2)$ and $C(x_3, y_3)$, $D(x_4, y_4)$ respectively. In this procedure, the height of the stair region is denoted by h, which value is $y_1 - y_2$ or $y_3 - y_4$. The ground height of stair region from top of the image plane is denoted by H, which value is$y_1 - y_p$ or $y_3 - y_p$. In this procedure, the vanishing point P is formed at the top of the image plane, so why it's y coordinate value y_p is zero. As a result, the value of H will be y_1 or y_3.

Assume that, the ratio of h and H is R, i.e. $R = \frac{h}{H}$. So, the value of R is $1 - \frac{y_1}{y_2}$ or $1 - \frac{y_3}{y_4}$, that is not dependent on the x and y coordinate value of vanishing point.

The vanishing point P is formed by the straight lines passing through the A, B, and C, D points. The straight line AB and CD are defined as $\frac{x-x_1}{x_1-x_2} = \frac{y-y_1}{y_1-y_2}$ and $\frac{x-x_3}{x_3-x_4} = \frac{y-y_3}{y_3-y_4}$ respectively. As the lines passing through the common point P (x_p, y_p), so the straight lines AB and CD will be $\frac{x_p-x_1}{x_1-x_2} = \frac{y_p-y_1}{y_1-y_2}$ and $\frac{x_p-x_3}{x_3-x_4} = \frac{y_p-y_3}{y_3-y_4}$ respectively.

Here, the value of h is equal to $y_1 - y_2$ *or* $y_3 - y_4$, and the value of H is equal to $y_p - y_1$ *or* $y_p - y_3$. Hence, the resultant AB and CD straight lines equation will be:

$$\frac{h}{H} = \frac{x_1 - x_2}{x_1 - x_p} \tag{3}$$

$$\frac{h}{H} = \frac{x_3 - x_4}{x_3 - x_p} \tag{4}$$

From Eqs. (3) and (4) we can write:

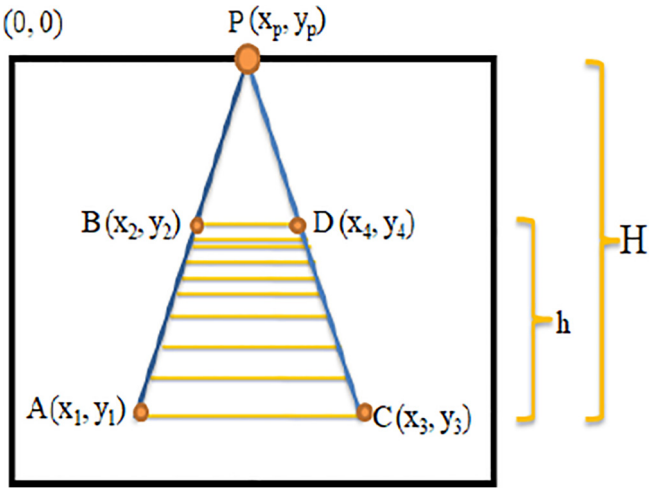

Fig. 18. Vanishing point location estimation procedure.

$$\frac{x_1 - x_2}{x_1 - x_p} = \frac{x_3 - x_4}{x_3 - x_p}$$

$$x_p = \frac{x_1 x_4 - x_2 x_3}{x_1 - x_2 - x_3 + x_4} \tag{5}$$

Assume that, the ratio of h, and H in Eqs. (3) and (4) is E. So, the value of E is: $\frac{x_1-x_2}{x_1-x_p}$ or $\frac{x_3-x_4}{x_3-x_p}$, where, x_p is the x coordinate value of the vanishing point P that is defined in Eq. (5). Here, the value of E depends on the x coordinate value of vanishing pointx_p.

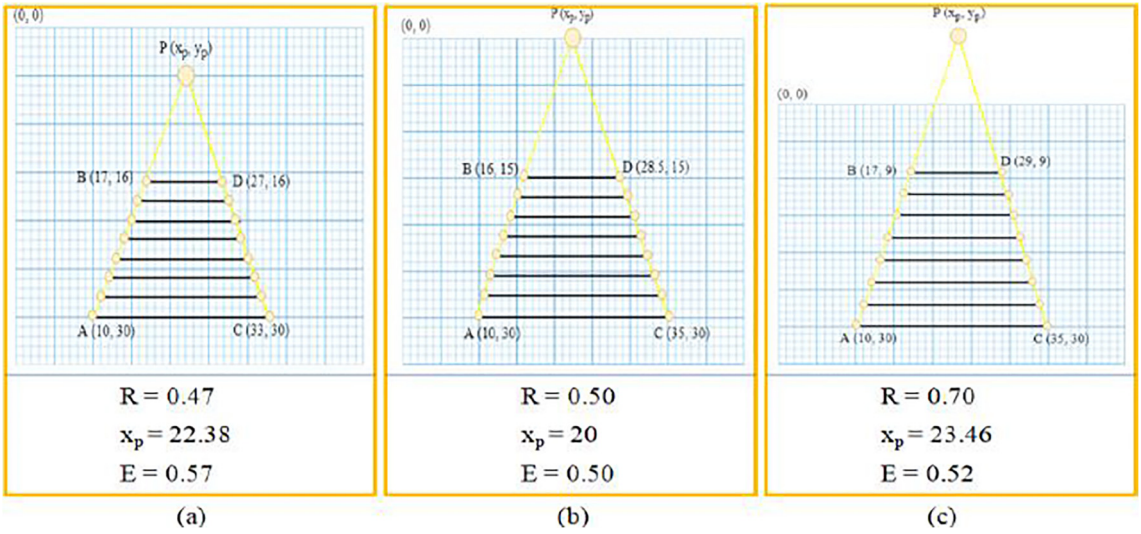

Fig. 19. Experimental analysis of vanishing point location based on the mathematical model: a) VP location within the image plane, where, R < E, b) the location of VP is at the border of the image plane, where, R = E, and c) the VP is located outside of the image plane, where, R > E.

According to the procedure shown in Fig. 18, the value of R and E will be the same as the vanishing point, P, resides at the border of the image plane. However, if the VP of stair region is resided within or outside of the image plane, in those situations these values i.e., R and E will not be same. This is because of the VP location within or outside of the image plane depends on the height of the stair region shown in Fig. 19. If the VP is located outside of the image plane in that situation the height (h) of the stair region will be increased, as a result, the value of R i.e. $R = \frac{h}{H}$ will be increased, which is shown in Fig. 19(c). On the other hand, if the VP is located within the image plane then the height (h) of the stair region will be decreased, so the value of R i.e. $R = \frac{h}{H}$ will be decreased, which is shown in Fig. 19(a). That means the value of R is proportional to the height of the stair region. Here, the value of E is changed by changing the value of vanishing point P as the value of E is dependent on the x coordinate value of P, where, the value of x_p depends on the x coordinate value of A, B, C, and D. The experimental analysis of the vanishing point location estimation procedure is demonstrated in Fig. 19.

From the mathematical and experimental analysis it is confirmed that the VP of stair region will be resided outside of the image plane if the value of R is greater than the value of E. On the other hand, the VP of stair region resides within the image plane when the value of R will be smaller than the value of E. The VP will reside in the border of the image plane when the value of R is equal to the value of E. The conditions are presented in Eq. (6).

$$VP\ location = \begin{cases} on\ the\ border\ of\ the\ image\ plane, & if\ R = E \\ Outside\ of\ the\ image\ plane, & if\ R > E \\ Inside\ of\ the\ image\ plane, & if\ R < E \end{cases} \tag{6}$$

3.3.3. Experimental justification

The experimental result regarding justifies the problem of VP is demonstrated in Fig. 20. Here, the demonstrated sample images are same as Sample 3, Sample 4, and Sample 5. However, these images are taken in a way that the camera is not focused on the stair region closely as well as the focal angle is bigger than the before. Here, Sample 7 is captured with the large focal angle, Sample 8 is captured with higher height from the ground, and Sample 9 is captured from the long distance. For these reasons, the slope and height of the stair regions seem to low as described in Figs. 15(b), 16(b), and 17(b). From the Fig. 20, it is seen that the y coordinate value of VP for Sample 7, Sample 8, and Sample 9 are 79.06, 18.84, and 69.34 respectively, which are not negative($y \geq 0$). For this regard, the stair candidate region is not verified through the y coordinate value of VP, although these samples i.e., Sample 6 in Fig. 14 and Sample 7, 8, and 9 in Fig. 20 are satisfied with the condition of stair geometrical features such as 3CP and sorted HEs.

The geometrical features validation and justification with VP and processing time for Sample 6 of Fig. 14 and Sample 7, 8, and 9 of Fig. 20 are presented in Table 2. The justification of the mathematical model for Sample 3, 4, 5 and Sample 7, 8, 9 are presented in Table 3.

From the above experimental analysis, it is revealed that the VP is not suitable to recognize and verify the stair candidate region from all scenarios. For this regard, the verification that is performed by the VP previously is verified through the SVM (Cortes and Vapnik, 1995). For that, the rotational invariant uniform local binary pattern (Lahdenoja et al., 2013) is used to extract the features from the stair candidate ROI.

3.4. Feature extraction and classification

To recognize the objects from the image through the classifier required to extract the appropriate features from the respective objects, which is an important part in the field of image recognition. For feature extraction, initially, the extracted object region is reshaped to 128 × 128. From that reshaped region features are extracted by using the uniform local binary pattern (Lahdenoja et al., 2013) with moment invariant ($LBP^{riu2}_{P,R}$) (Ojala et al., 2002). The $LBP^{riu2}_{P,R}$ is a extended version of the LBP (Pietikäinen et al., 2011; Hou, 2003 used to describe the target feature due to its low computational complexity. The $LBP^{riu2}_{P,R}$ is define in Eq. (7) (Lahdenoja et al., 2013; Hou, 2003).

$$LBP^{riu2}_{P,R} = \begin{cases} \sum_{h=0}^{p-1} s(g_h - g_c), & if\ U(LBP_{P,R}) \leq 2 \\ P + 1 & otherwise \end{cases} \tag{7}$$

Where,

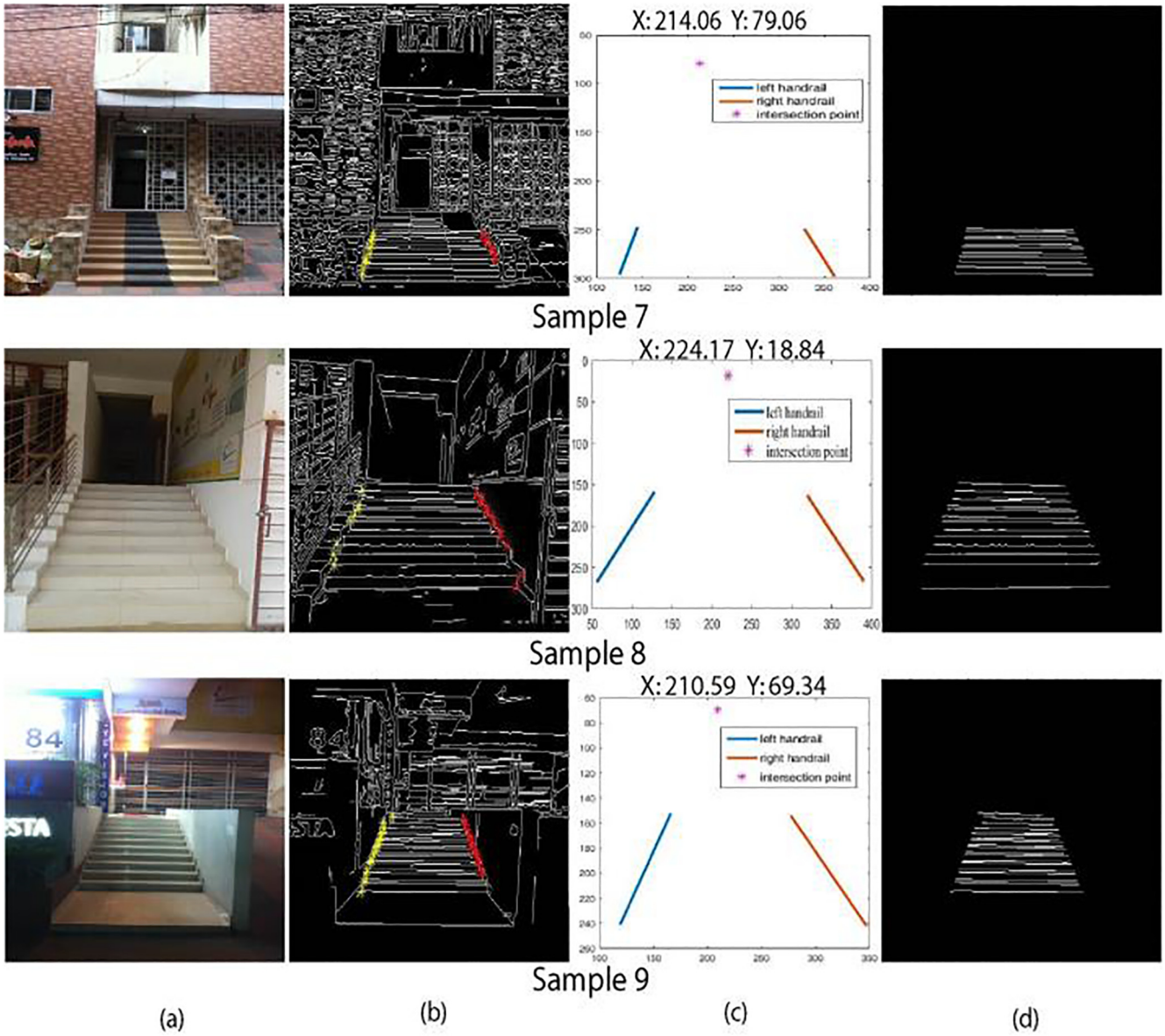

Fig. 20. Processing example of stair samples to identify the VP's problem: a) input stair RGB image, b) HEs validated by 3CPs, c) estimating the vanishing point, where, y≥0, and c) HEs are in sorted order.

Table 2
Validated stair step HEs by 3CPs, estimating VP value, and the processing time of sample images presented in Figs. 14 and 20.

Stair Sample	Total HE	Total 3CP	3CP (%)	Vertical VP	Run time (s)
6	15	14	93.33	(229.36, 23.85)	0.059
7	12	11	91.67	(214.06, 79.06)	0.060
8	14	11	78.57	(224.17, 18.84)	0.056
9	18	15	83.33	(210.59, 69.34)	0.063

$$U(LBP_{P,R}) = \left|s(g_{p-1} - g_c) - s(g_0 - g_c)\right| + \sum_{h=1}^{p-1} \left|s(g_h - g_c) - s(g_{h-1} - g_c)\right| \quad (8)$$

here, the uniformity measure U corresponds to the number of spatial transitions, i.e., changes between 0 and 1 in the pattern. The g_c is the gray value of the center pixel (x, y) and g_h is the neighboring of P pixel with radius R. The sign function $s(z)$ of a sequence z is defined in Eq. (9).

$$s(z) = \begin{cases} 1, if\ z \geq 0 \\ 0, otherwise \end{cases} \quad (9)$$

The uniform patterns are achieved from the $LBP^{riu2}_{P,R}$ for two transition between 0 and 1 bit is 59 for P = 8 and R = 1 neighborhood. That is because of, for P = 8 there are seven set of codes with an increasing number of 1, i.e., 00000001, 00000011, …, 011111111. Each of these set has 8 combinations. For example, 00,000,001 has 8 combinations, such as, 10000000, 01000000, 00100000, 00010000, 00001000, 00000100, 00000010, and 00000001. So,

Table 3
Justification of stair region's VP location based on the value of R and E.

Stair sample	*x*coordinate value of A, B, C, and D point				*y*coordinate value of A, B		Value of x_p	Value of R	Value of E	VP's position
	x_1	x_2	x_3	x_4	y_1	y_2				
3	47	118	375	316	237	49	226.14	0.79	0.39	Outside of the image plane
4	65	132	390	313	258	106	216.22	0.59	0.44	
5	37	145	433	342	230	99	251.91	0.57	0.50	
7	125	145	361	328	269	247	214.06	0.08	0.22	Inside of the image plane
8	56	128	390	319	269	159	224.17	0.41	0.43	
9	119	166	347	277	241	152	210.59	0.37	0.51	

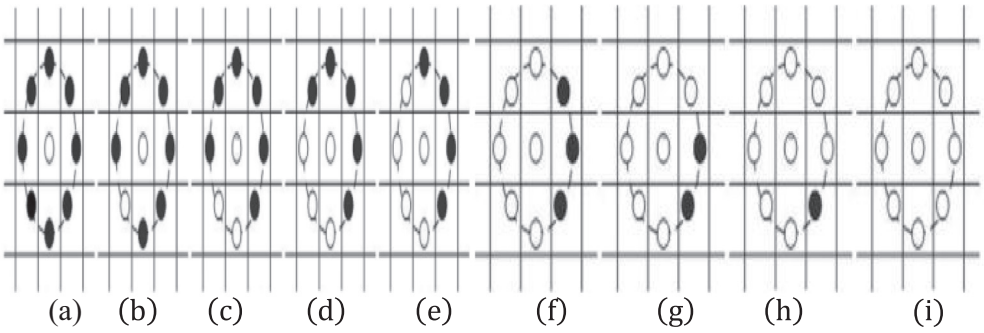

Fig. 21. Uniform patterns of $LBP^{riu2}_{P,R}$ for P = 8 and R = 1: a) spot, b) spot, c) line end, d) corner, e) edge, f) corner, g) line end, h) spot/flat, and i) spot/flat.

Fig. 22. Various types of positive stair images: a) indoor stair with different illumination, b) and c) outdoor stair with different illumination noisy backgrounds.

Fig. 23. Different types of negative stair images with the similar visual pattern.

the total number of output labels is $8 \times 7 = 56$. For the uniform binary patterns there exist three additional combinations. The combinations are 00000000, 11111111 and one for all non-uniform patterns. So, the total number of output label is $8 \times 7 + 3 = 59$, i.e., $P \times (P - 1) + 3$.

Moreover, uniform LBP is used in this work to describe the target features that are produced better recognition results. The $LBP^{riu2}_{P,R}$ patterns of an object are shown in Fig. 21. Here, the black and white circle represents the bit value of zero and one. The $LBP^{riu2}_{P,R}$ model extracts the primal including edges, corners, lines, flat areas, as well as spots. Where, edge, line, and corners are major uniform patterns. Finally, the extracted features are classified through the SVM (Burges, 1998; Cortes and Vapnik, 1995).

4. Experimental results and discussions

The processing example and discussion of the experimental result are presented in this section. All the experiments presented in this paper are made with Intel (R) Xeon (R) CPU E31220@3. 10GHZ. The RAM used in the PC is 4 GB. In the experiments, the images used are sized on 480×320. After extracting the stair ROI, the candidate region is reshaped to 128×128 pixels. The experiments demonstrate in the MATLAB environment.

4.1. Used dataset

The images that are used in this paper are our own created dataset those are collected from the different scenario with different illumination and noisy conditions. A total of 251 stair images are used in the dataset. However, this dataset is separated by two datasets those are training and testing dataset. In the training data set, 138 stair images are used, where 116 stair images are utilized in the testing dataset. Some positive stair samples are presented in Fig. 22 and negative images with the similar visual pattern of the stair are presented in Fig. 23.

4.2. Processing examples

This section presents some processing example of stair detection from different environments and illumination conditions. The detected stair candidate region is recognized through the SVM classifier. The processing examples are demonstrated in Fig. 24. Where, Sample 10, 11, and 12 are taken with low illumination and noisy conditions from the indoor environment. Where, the stair Sample 12 is an elevator. Some samples are taken from the outdoor scenarios with different lighting conditions at night and day times, i.e. Sample 13, and 14. From the experimental results shown in Fig. 24 elicit that the stair detection method efficiently detects the stair candidate region from the different environment and illumination condition through the geometrical features of the stair.

Fig. 25 shows some experimental results of the complex stair images that are captured from the indoor environments i.e., Sample 16 and outdoor environments i.e., Sample 15 and 17. From stair Sample 15 and 17, it is seen that the surrounding environment of the stairs contains complex information such as trees and grasses. It is also observed that the frontal stair steps are fully visible; however, after a certain distance, the further portions of the stair steps are not visible properly. That is because of, a further portion of the stair steps is in-depth and narrow, as well as depth edges of stair steps are not determined to compare to the frontal edge segment.

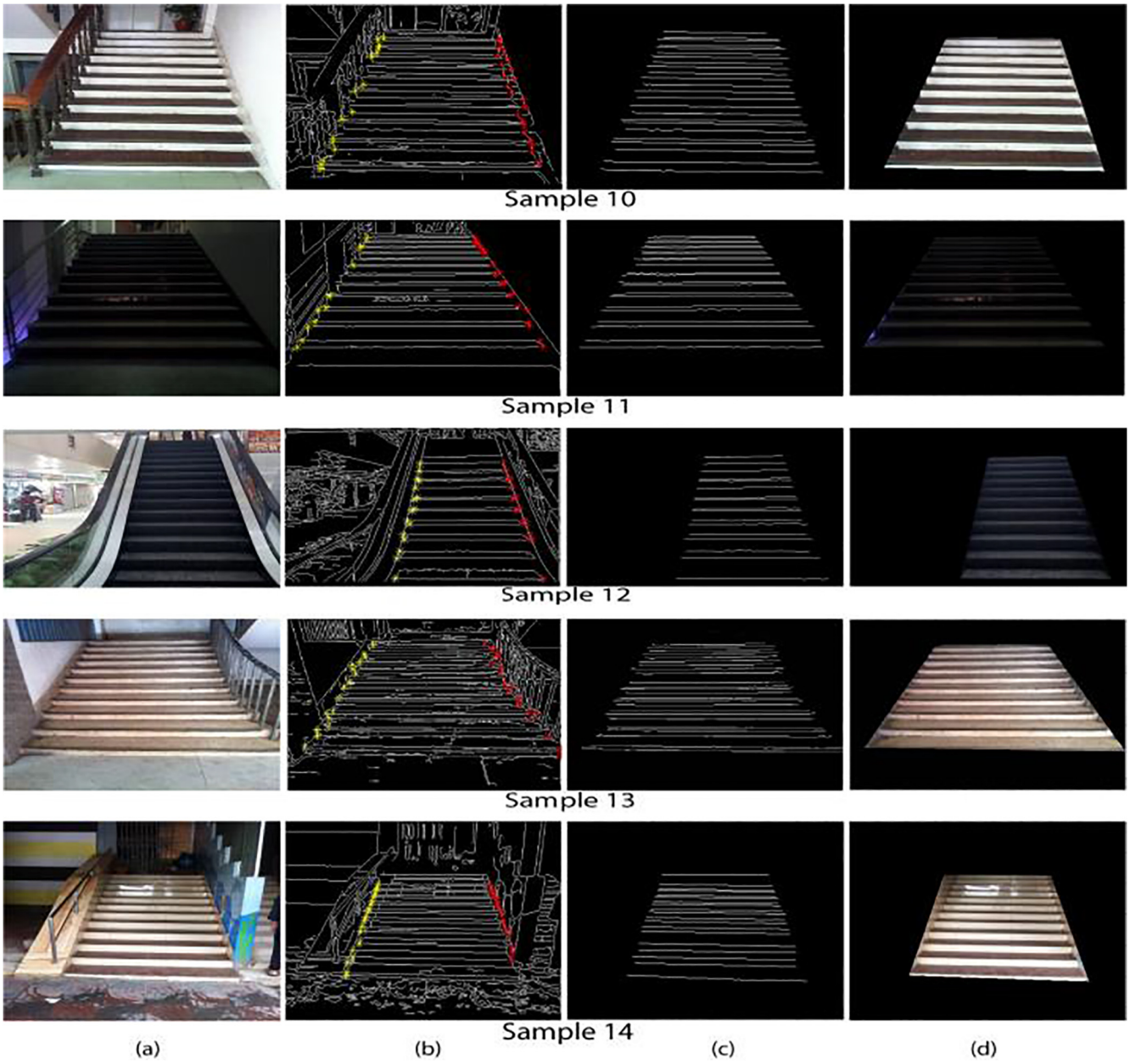

Fig. 24. Processing example of stair region detection by geometrical features and recognized by SVM: a) input stair RGB image, b) HEs validated by 3CPs, c) HEs are in sorted order, and d) extracted stair candidate ROI.

As the further portion of the stair step's edge segment is not determined properly, that portion of the stair region is not detected appropriately. The other stair Sample 16 is captured from the indoor scenario with a noisy background. In which shadows are fall in the different portion of the image. The noisy and shadow's effects are eliminated by the filter and extract the appropriate stair-step edges from the input image.

Fig. 26 shows the various processing examples of the stair that are taken at the different orientations. These samples are also satisfied with the conditions of geometrical features and VP conditions as like the normal oriented stair images.

However, some conditions have to be satisfied in the phase of capturing the different oriented stair images. The conditions are that the camera should be placed in the stair region's horizontal axis. The displacement of stair region's angular orientation should be below 30^0. It is seen that by the proposed framework the stair steps horizontal and vertical edges are detected effectively and extract the stairways ROI efficiently through the geometrical features and recognize by using SVM.

4.3. Discussions

The performance of the proposed system is measured by using the different scenarios stair images. The performance is measured by utilizing machine learning feature matrices such as precision, recall, and F1-score. These values are estimated by using the true positive (TP), false positive (FP), true negative (TN) and false negative (FN) values. The true positive is the result that the proposed method correctly detected from the stair region. The true negative is the result that the proposed system correctly detects as a non-stair region. The false positive is the result that the proposed system shows the non-stair region, where the stair candidate region

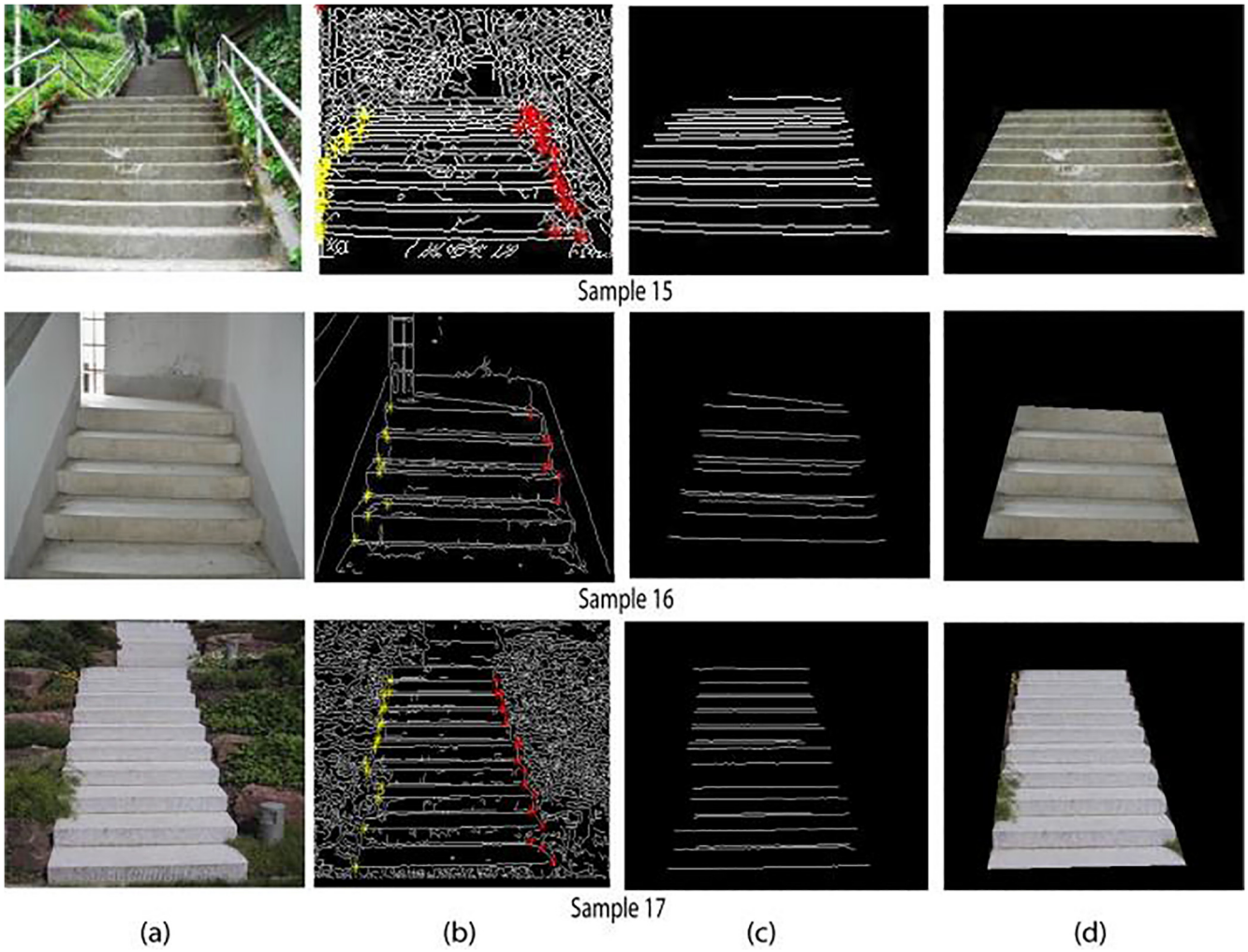

Fig. 25. Processing example of detecting stair region in complex scenarios: a) input stair RGB image, b) HEs validated by 3CPs, c) HEs are in sorted order, and d) extracted stair candidate ROI.

is exited. The false negative is the result that the proposed system shows the stair region where the candidate stair region does not exist.

The recall refers to the completeness of the proposed method. It indicates that what percent of correct stair region is detected by the proposed method as such. Where, precision refers to the exactness of the proposed method. It indicates that what percent of stair region is correctly detected by the proposed method is actually such. The recall and precision are defined by Eqs. (10) and (11) respectively. The F1-score is defined as the harmonic mean of the recall and precision. The F1-score is defined by Eq. (12).

$$\text{Recall} = \frac{\text{TP}}{\text{TP} + \text{FP}} \tag{10}$$

$$\text{Precision} = \frac{\text{TP}}{\text{TP} + \text{FN}} \tag{11}$$

$$\text{F1} - \text{Score} = 2.\frac{\text{Recall.Precesion}}{\text{Recall} + \text{Precision}} \tag{12}$$

The effectiveness of the proposed method for detecting the stair ROI is shown in Table 4. The verification accuracy with respect to the VP and SVM classifier is presented at Table 5. The proposed method is compared with Khaliluzzaman and Deb (2018), Wang et al. (2014), Deb et al. (2013) and Hernandez and Jo (2010) with respect to average detection accuracy and computation time are presented in Table 6. The accuracy of stair ROI detection by the proposed stair detection framework is calculated using Eq. (13).

$$\text{Stair detection accuracy} = \frac{\text{TP} + \text{TN}}{\text{TP} + \text{TN} + \text{FP} + \text{FN}} * 100\,\% \tag{13}$$

In Khaliluzzaman and Deb (2018), the directional Gabor filter is used to filter the input image which performance depends on the appropriate selection of parameters i.e., Gaussian variance, orientation, and wavelength. For that reason, a set of parameter is considered to get the best response from the noisy image. In that framework, small edges are removed from the edge image through the heuristic threshold value which is not working well for all the experiments with different scenarios. Furthermore, 3CP is used to validate the stairways edges and extract the sorted HEs by comparing the x coordinate values of consecutive edges end points. Finally, stair HE segment is verified through the y coordinate value of VP, which is negative, i.e. $y < 0$. However, the y coordinate value of VP does not verity the different scenario's stair candidate region for various reasons that are justified in Section 3.3.

In Wang et al. (2014), the authors used the depth information to detect and recognize the stair images. However, the system is not working better in the outdoor environment where light intensity is high. That is because of the depth sensor is not able to detect the depth information properly where sunshine is too bright. The

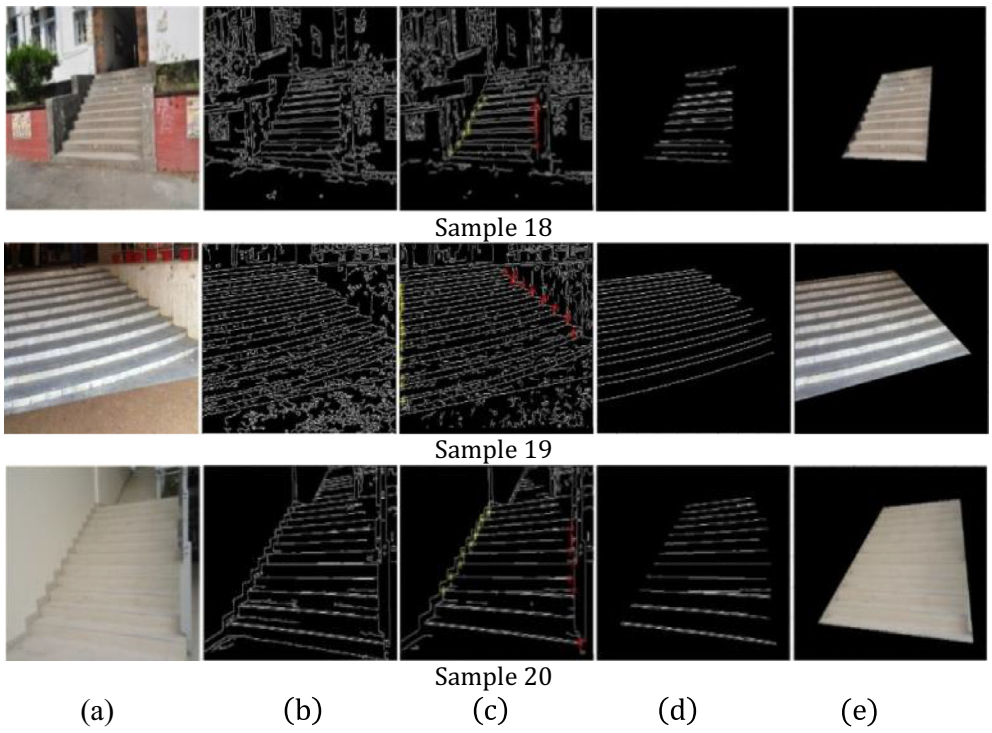

Fig. 26. Processing example of detecting stair region in various orientation: a) input stair RGB image, b) Canny edge image, c) HEs validated by 3CPs, d) HEs are in sorted order, and e) extracted stair candidate ROI.

Table 4
Performance accuracy of stair proposed method in the case of detecting stair ROI.

Stair type	Total images	Detection error				Precision (%)	Recall (%)	F1- Score
		TP (%)	FP (%)	TN (%)	FN (%)			
Indoor	48	98.12	2.04	97.96	1.88	97.96	98.12	98.04
Outdoor	68	96.44	3.15	96.85	2.56	96.85	97.44	97.14
Overall performance	**116**	**97.28**	**2.60**	**97.40**	**2.22**	**97.40**	**97.78**	**97.59**

Table 5
Performance accuracy of the proposed method in the case of verifying stair ROI by SVM and VP.

Stair type	Total image	No of images correctly verified		Detection error		Verification accuracy (%)	
		VP	SVM	VP	SVM	VP	SVM
				FP (%)	FP (%)		
Indoor	48	47	48	2.17	0.50	97.83	99.50
Outdoor	68	66	67	3.02	1.21	96.98	98.79
Overall performance	**116**	**113**	**115**	**2.60**	**0.86**	**97.40**	**99.14**

Table 6
Comparison of the proposed method.

Method	Accuracy (%)	Avg. run time (s)
The proposed method with VP	**97.40**	**0.061**
The proposed method with SVM	**99.14**	**0.055**
Khaliluzzaman et al.	97.12	0.067
Wang at al.	97.16	0.200
Deb et al.	96.15	0.085
Hernandez et al.	93.83	0.149

RGB-D image is also not able to extract the depth information appropriately from the low illumination conditions.

In Deb et al. (2013), the authors use the dynamic programming to extract the horizontal edges which appear in increasing subsequent order. This HE segment is estimated from the horizontal edge image by utilizing heuristic threshold value, which is not suitable for all the experiments. There would be some horizontal edges that are not part of the parallel concurrent horizontal edges. The longest horizontal edges may have some break or horizontal gap. Still, these horizontal edges are represented a single horizontal edge. In this framework, the authors have not considered these types of situations. The horizontal edges are arranged in the longest increasing subsequence by applying the longest increasing subsequence algorithm. This method takes $O(n \log n)$ time to solve this issue. Finally, the detected candidate region is recognized by the vertical VP. However, the vertical VP does not recognize the stair candidate region from all the scenarios and not able to differentiate the stair region from other analogous object. The regions are elaborately explained in the Section 3.3.

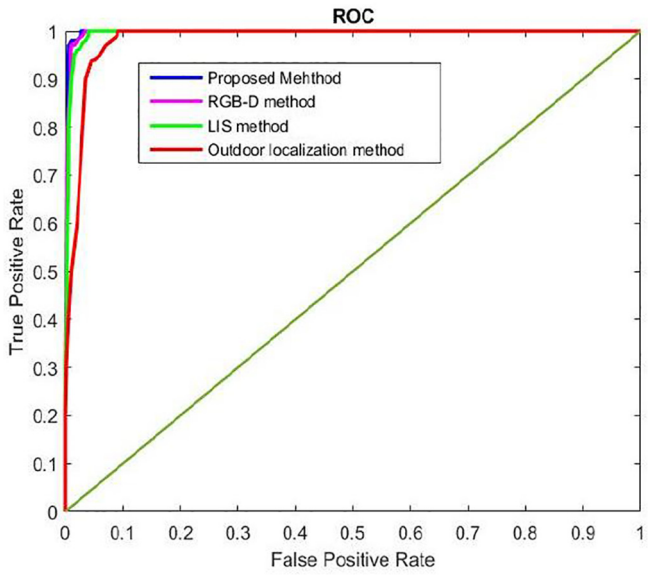

Fig. 27. ROC curve for proposed method compared with RGB-D method (Wang et al., 2014), LIS method (Deb et al., 2013), and outdoor localization method (Hernandez and Jo, 2010).

In Hernandez and Jo (2010), outdoor stairway candidate region is located through the angle of the stair and vertical VP. The stairway angle and VP are determined based on the stairway handrails. However, every entire stairway in the outdoor environment does not contain the handrail and some stairway contains one side of the handrail. So, those stairways that do not contain both sides of handrails of the stairways are not detected by this method. In addition to this, the method proposed in Deb et al. (2013) localized the stair candidate region first then detect the stair candidate region from the detected localization area. The stair area is localized by the y coordinate value of vertical vanishing point which is negative, i.e.$y < 0$. However, the y coordinate value of VP does not localize the different scenario's stair candidate area for various reasons that are justified through the three basic criteria and a mathematical model.

In this paper, a method is proposed to detect the stair candidate region with the key features of three connected point and stair HEs are in sorted increasing order. The three connected points are estimated from the stair edge image and used to extract the increasing HEs without comparing the y coordinate values of consecutive edges end points. This problem is solved within $O(n)$ time, which is linear, where; n is the number of horizontal parallel edges of the stair. In the proposed method MSVD is used to eliminate the influence of eliminations of the stair image and extract the different oriented stair edges from different environmental conditions. The MSVD is performed by decomposing the input image into four sub bands i.e., Image $(4, :)$. Where, Image $(1, :)$ contains the approximation components and signal information of image. In this method, specific parameters do not need to consider as like the Gabor filter. The approximation components are estimated automatically through the large Eigen values describe in Section 3.1. Potential horizontal edges are extracted by utilizing an edge elimination procedure, where the statistical threshold value is used. Non-parallel horizontal edges are eliminated by using a non-candidate edge elimination procedure. And longest HEs are extracted through the edge linking and tracking procedure. After

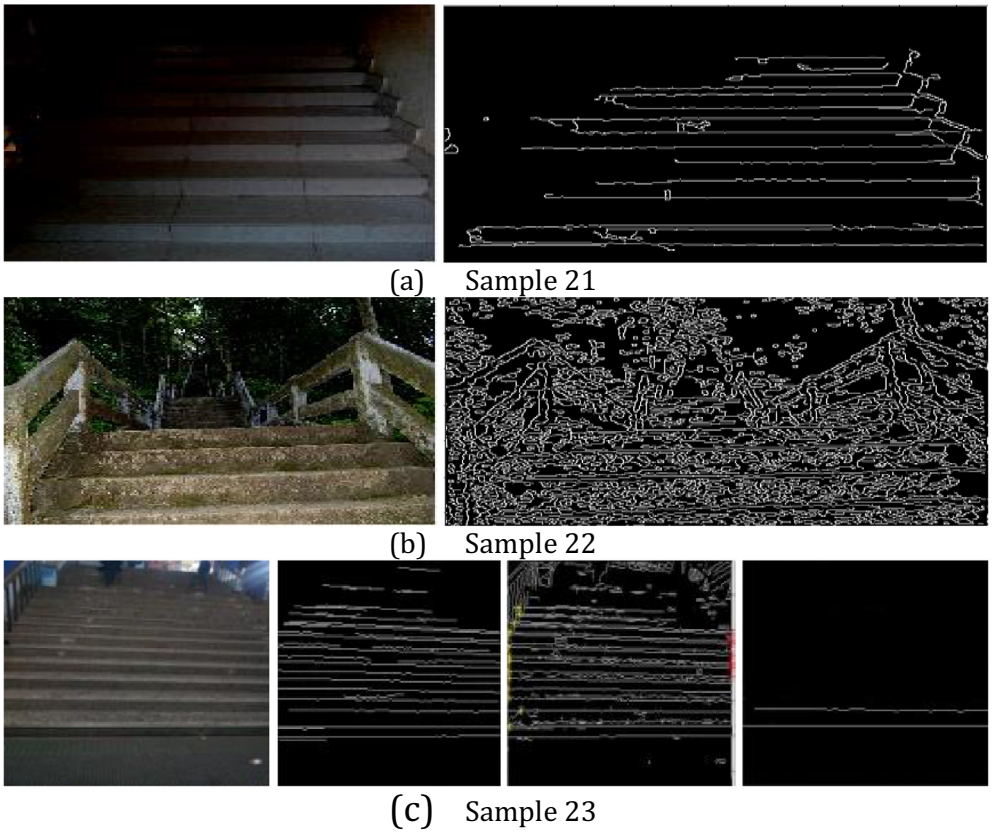

Fig. 28. Sample stair images from where the proposed method failed to detect the stair candidate region: (a), (b), and (c) stair image where the stair detection method failed to detect the stair candidate region.

that, investigate the problem of VP which is used for the stair region verification. Finally, justify the problem of VP with the experimental result based on the three basic criteria and a mathematical model. Finally, SVM classifier is used to perform the verification. For classification, the rotational invariant uniform local binary pattern features are used.

The Receiver Operating Characteristic (ROC) curve for the proposed method compared with RGB-D method (Wang et al., 2014), LIS method (Deb et al., 2013), and outdoor localization method (Hernandez and Jo, 2010) is shown in Fig. 27. Fig. 28 shows the result of some stair sample images in which stair detecting method is failed to detect stair candidate region due to poor image resolution, overexposure, circumventions, blur in the image, different structure of the stair, and change of viewpoints during capturing of the image etc.

In Fig. 28, stair Sample 21 is captured from the indoor environment where one side of the image is too noisy. Due to the high noise in the one side of the stair image, the stair detection framework is not able to detect the stair step edges in that portion. For that reason, the three connected points are not extracted from that portion. As the three connected points are not extracted from the edge image, the proposed stair detection framework is not able to detect the stair candidate region from this type of stair image.

Stair Sample 22 which is captured from the noisy and blur environment where the image body is not sharp. From that image, it is seen that it is difficult to detect the horizontal and vertical edges from the edge image. The stair region is detected by the proposed stair detection framework through the natural and unique property of three connected point. For satisfying these properties the vertical and horizontal edges are required to be extracted from the stair edge image that is represented in Fig. 28(b). Moreover, stair Sample 23 which is captured from the outdoor environment, this stair is captured partially and satisfied the condition of 3CP. However, upper horizontal edges are bigger than the lower horizontal edges. For that, edges do not appear in sorted sequential order and not justify the condition of stair step edges.

5. Conclusion

This paper presents a stair detection method based on the aforementioned geometrical feature of the stair with justifying the vanishing point problem in the phase of stair candidate region verification. This method is important to understand the problem of the vanishing point in the phase of stair region verification at different scenarios, which being its strong point. This method is also important to navigate the autonomous system in obscure environments. The proposed method is tested with various noisy and oriented images to justify the efficiency and effectiveness of the method. This proposed method shows its effectiveness in the processing time and detection accuracy of 0.061(s) and 97.58% respectively. This method also justified the problem of VP in the phase of stair region verification with the three basic criteria and a mathematical model. The three basic criteria used in this paper are focal angle of the camera, height of the camera from the ground, and distance of the camera from the stair image. Where, the mathematical model estimates the location of the VP of the stair region to predict whether the VP is resided within or outside of the image plane. Finally, the SVM classifier is used instead of VP to verify the stair candidate region. The experimental results elicit that the SVM classifier presents improved accuracy with compare to the VP. The proposed method is limited to detect the stair with usual shapes such as a spiral stair. This is because of the proposed system detects the stair ROI through the geometric feature of the stair. This type of feature does not exist in the spiral staircases. In future, the proposed method will be updated to detect the stairways from the unusual stair shapes.

References

Barnard, S.T., 1983. Interpreting perspective images. Artif. Intell. 21 (4), 435–462.

Basca, C.A., Brad, R., 2007. Texture segmentation. Gabor filter bank optimization using genetic algorithms. In: Proceeding of the International Conference on Computer Tool. IEEE. pp. 331–335.

Burges, C.J., 1998. A tutorial on support vector machines for pattern recognition. Data Min. Knowl. Disc. 2 (2), 121–167.

Cong, Y., Li, X., Liu, J., Tang, Y., 2008. A stairway detection algorithm based on vision for ugv stair climbing. In: Proceeding of the IEEE International Conference on Networking, Sensing and Control (ICNSC). IEEE. pp. 1806–1811.

Cortes, C., Vapnik, V., 1995. Support-vector networks. Mach. Learn. 20 (3), 273–297.

Deb, K., Islam, S.T., Sultana, K.Z., Jo, K.H., 2013. Stairway detection based on extraction of longest increasing subsequence of horizontal edges and vanishing point. In: Contemporary Challenges and Solutions in Applied Artificial Intelligence. Springer, pp. 213–218.

Du Buf, J.H., Barroso, J., Rodrigues, J.M., Paredes, H., Farrajota, M., Fernandes, H., José, J., Teixeira, V., Saleiro, M., 2011. The SmartVision navigation prototype for blind users. Int. J. Digital Content Technol. Appl. (JDCTA) 5 (5), 351–361.

Harms, H., Rehder, E., Schwarze, T., Lauer, M., 2014. Detection of ascending stairs using stereo vision. In: Proceeding of the 2014 IEEE International Symposium on Innovations in Intelligent Systems and Applications (INISTA). IEEE. pp. 313–318.

Harms, H., Rehder, E., Schwarze, T., Lauer, M., 2015. Detection of ascending stairs using stereo vision. In: Proceeding of the 2015 IEEE/RSJ International Conference on Intelligent Robots and Systems (IROS). IEEE. pp. 2496–2502.

Hernandez, D.C., Jo, K.H., 2010. Outdoor stairway segmentation using vertical vanishing point and directional filter. In: Proceeding of the International Forum on Strategic Technology. IEEE. pp. 82–86.

Hernández, D.C., Kim, T., Jo, K.H., 2011. Stairway detection based on single camera by motion stereo. In: International Conference on Industrial Engineering and Other Applications of Applied Intelligent Systems. Springer, pp. 338–347.

Hou, Z., 2003. Adaptive singular value decomposition in wavelet domain for image denoising. Pattern Recogn. 36 (8), 1747–1763.

Huertas, A., Medioni, G., 1986. Detection of intensity changes with subpixel accuracy using Laplacian-Gaussian masks. IEEE Trans. Pattern Anal. Mach. Intell. 5, 651–664.

José J, Rodrigues, J.M., du Buf, J.M., 2012. Visual navigation for the blind: path and obstacle detection. In: 2012 International Conference on Pattern Recognition Applications and Methods. pp. 515–519.

Khaliluzzaman, M., Deb, K., 2016. Support vector machine for overcoming the problem of vanishing point during stairways detection. In: International Conference on Electrical, Computer & Telecommunication Engineering (ICECTE). IEEE. pp. 1–5.

Khaliluzzaman, M., Deb, K., 2018. Stairways detection based on approach evaluation and vertical vanishing point. Int. J. Comput. Vis. Rob. Indersci. 8 (2), 168–189.

Lahdenoja, O., Poikonen, J., Laiho, M., 2013. Towards understanding the formation of uniform local binary patterns. In: ISRN Machine Vision.

Lee, Y.H., Leung, T.S., Medioni, G., 2012. Real-time staircase detection from a wearable stereo system. In: Proceeding of the 21st International Conference on Pattern Recognition (ICPR). IEEE. pp. 3770–3773.

Mäenpää, T., Pietikäinen, M., 2005. Texture analysis with local binary patterns. Handb. Pattern Recognit. Comput. Vis., 197–216

Mallat, S.G., 1989. A theory for multiresolution signal decomposition: the wavelet representation. IEEE Trans. Pattern Anal. Mach. Intell. 11 (7), 674–693.

McLean, G.F., Kotturi, D., 1995. Vanishing point detection by line clustering. IEEE Trans. Pattern Anal. Mach. Intell. 17 (11), 1090–1095.

Naidu, V.P.S., 2011. Image fusion using multi-resolution singular value decomposition. Defence Sci. J. 61 (5), 479–489.

Ojala, T., Pietikainen, M., Maenpaa, T., 2002. Multiresolution gray-scale and rotation invariant texture classification with local binary patterns. IEEE Trans. Pattern Anal. Mach. Intell. 24 (7), 971–987.

Pietikäinen, M., Hadid, A., Zhao, G., Ahonen, T., 2011. Computer Vision using Local Binary Patterns. Springer, p. 40.

Schaffalitzky, F., Zisserman, A., 2000. Planar grouping for automatic detection of vanishing lines and points. Image Vis. Comput. 18 (9), 647–658.

Schwarze, T., Zhong, Z., 2015. Stair detection and tracking from egocentric stereo vision. In: Proceeding of the 2015 IEEE International Conference on Image Processing (ICIP). pp. 2690–2694.

Shahrabadi, S., Rodrigues, J.M., Du Buf, J.H., 2013. Detection of indoor and outdoor stairs. In: Iberian Conference Pattern Recognition and Image Analysis. Springer, pp. 847–854.

Wang, S., Pan, H., Zhang, C., Tian, Y., 2014. RGB-D image-based detection of stairs, pedestrian crosswalks and traffic signs. J. Vis. Commun. Image Represent. 25 (2), 263–272.